N71-35506

NASA CR-111910

Final Report

DESIGN, FABRICATION AND EVALUATION OF A PROTOTYPE MOLECULAR BEAM GIMBALLED DETECTOR, CONTROL CIRCUITS, AND SIGNAL PROCESSING ELECTRONICS

By Wallace S. Kreisman

Prepared under Contract No. NAS1-8223 Task 5

NATIONAL RESEARCH CORPORATION
Cambridge, Massachusetts

for

NATIONAL AERONAUTICS AND SPACE ADMINISTRATION

TABLE OF CONTENTS

LIST OF ILLUSTRATIONS

DESIGN, FABRICATION AND EVALUATION OF A PROTOTYPE MOLECULAR BEAM GIMBALLED DETECTOR, CONTROL CIRCUITS, AND SIGNAL PROCESSING ELECTRONICS

by Wallace S. Kreisman
National Research Corporation
Cambridge, Massachusetts 02142

SUMMARY

For some time, a need has existed to develop an accurate method of measuring active gaseous species, such as atomic oxygen, in either the Earth's upper atmosphere or the atmospheres of other planets. Active gaseous species tend to recombine or interact chemically with other elements when they strike a surface. Due to our inability to predict the degree of recombination or chemisorption, measurements of gases such as atomic oxygen can have large uncertainties.

Because measurements of upper atmosphere gases are made from high speed vehicles such as rockets and satellites, it is possible to make use of the vehicle velocity to create a "molecular beam" of unscattered ambient atoms and molecules. A molecular beam can be created by aligning two or more orifices or skimmers in the direction in which the vehicle is moving. A gimballed orifice (sampler) and detector system, together with vehicle attitude information, can maintain alignment.

This report describes a gimballing system that was designed and constructed to permit a beam-forming sampler and mass spectrometer detector to be moved $\pm$ 25° in both pitch and yaw in a vacuum environment. The basic elements of the instrument weigh about 5 lbs., take about 12 watts of peak power, have angular position accuracies of about 1 degree and have speeds of response of less than 1 second.

INTRODUCTION

In making measurements of the Earth's atmosphere or other planetary atmospheres from satellites and space vehicles, it is important to obtain representative samples that have not been modified by either the vehicle or the measurement instrument itself. For example, atmospheric composition measurements can be made with the use of a free molecular flow inlet system and a mass spectrometer as recently proposed[1]. Such a system minimizes gas-wall collisions of the ambient atoms and molecules before they are ionized and analyzed.

The use of a molecular beam sampler inlet system with its associated skimmers requires a zero angle of attack attitude. For a satellite that does not contain a stable platform, zero angle of attack may be obtained by using a properly designed gimballing system. The orientation sensors required to align a gimballed system can be ambient ion sensors of the type recently developed.[2]

The current program has been concerned with the design, construction and testing of a gimballed system that can be mounted on a space vehicle for the purpose of aligning some instrument (such as a molecular beam sampler and mass spectrometer) with the relative wind. The gimballed system receives an input signal from ion sensors or equivalent vehicle orientation sensors and rotates in pitch and yaw to bring the measurement instrumentation to some desired position with respect to the vehicle relative velocity vector. The same type of gimballed system can also be used to orient an instrument with respect to some object in space if the appropriate orientation input signals are furnished.

The basic characteristics of the gimballed detector can be listed as: 1) Small size, 2) Low power, 3) Low weight, 4) Operation in a vacuum environment, 5) Low outgassing, 6) Essentially vacuum enclosed, 7) Limited movements in pitch and yaw, 8) Angular position accuracies of the order of 1 degree, 9) Speed of response of the order of 1 second.

As shown in Figure 1, the gimballed detector consists of several basic elements. The heart of the system is the ball bearing supported gimbals which hold the detector instrumentation. Small torque motors are mounted on the gimbal structure to move the detector in pitch and yaw. Feedback potentiometers are also mounted on the gimbal structure to sense the position of the detector. The actual position of the detector is compared with the desired position and the difference or error signal is amplified by the torque amplifiers and converted to a driving signal input to the torque motors. Compensating phase lead network filters are used to improve the system response.

Physically, the gimballed detector system is enclosed in a cylindrical vacuum envelope as shown in Figure 2. A spherical gap, low vacuum conductance seal at the front of the unit permits the detector to be moved in yaw and pitch without constraint while still maintaining an acceptable vacuum within the envelope. In operation, the front end of the system is sealed with a break-off device and is not opened to the ambient air until measurements are to be made at high altitudes (i.e., under high vacuum conditions).

In addition to the mechanical elements of the gimballed system and its electrical control unit, a signal processing electronics package was designed and constructed to accept

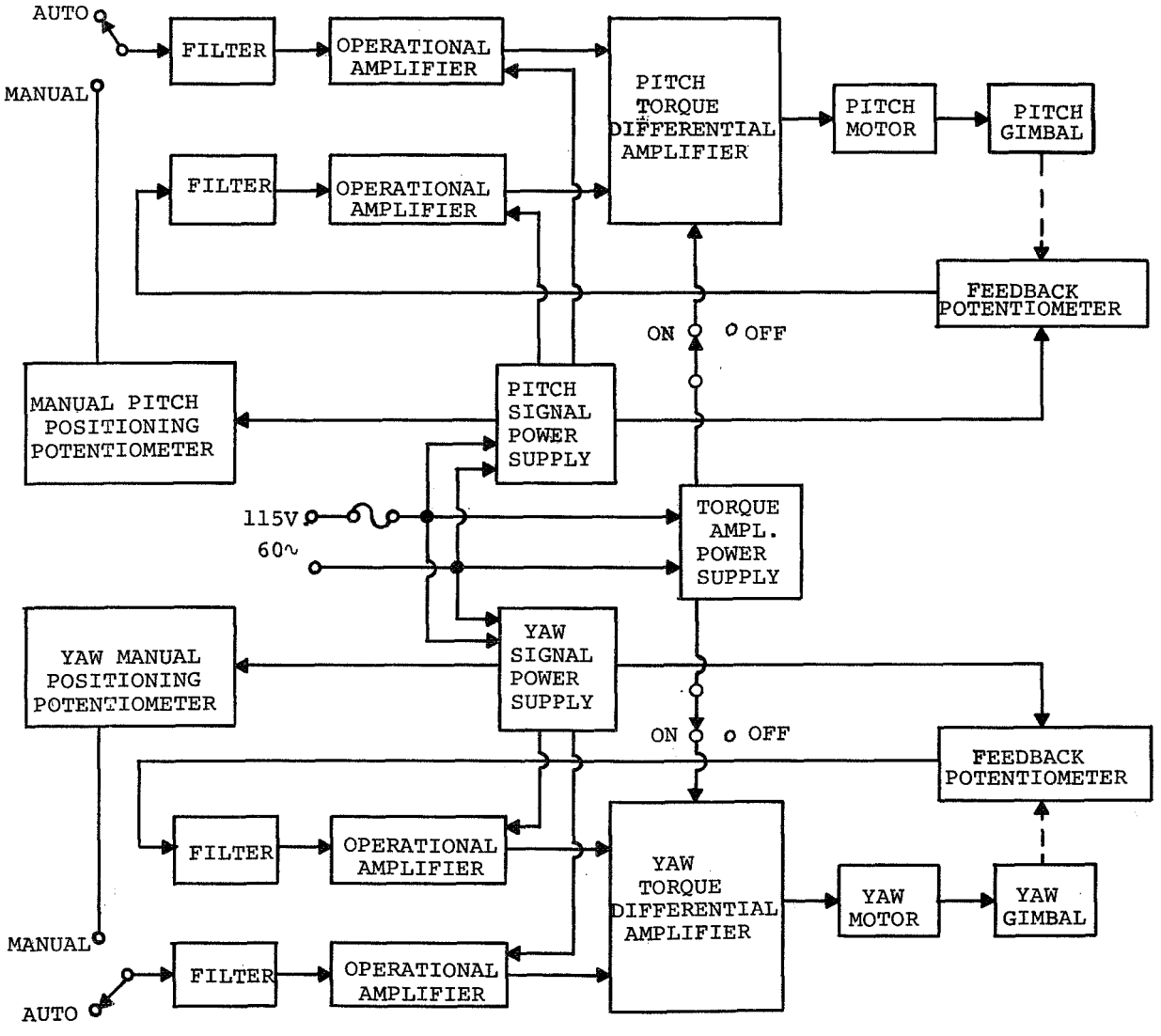

Figure 1. Block Diagram of Gimballed Detector Servo System.

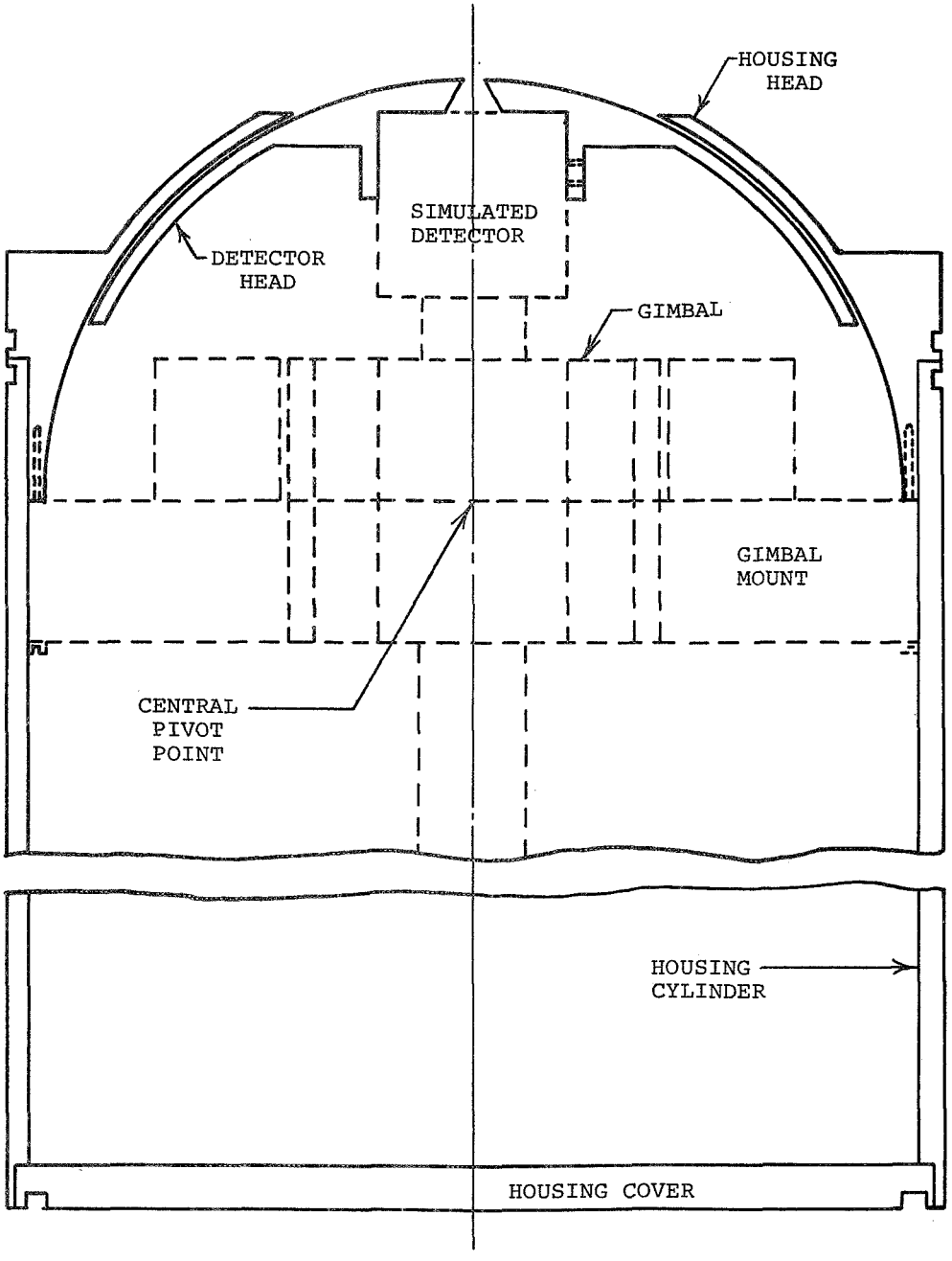

Figure 2. Sketch of Enclosed Gimballed Detector.

analog data voltages from an actual gimballed detector (quadrupole mass spectrometer), multiplex the voltages, and convert the analog voltage values to digital form suitable for telemetry. A block diagram of the signal processing electronics is shown in Figure 3. The functions of the various elements of this system will be described in later sections.

The following sections of this final report deal with the design, construction and testing of the gimballed detector system and the associated signal processing electronics. Sufficient information was obtained to evaluate the performance of the system.

THEORY

As can be seen from the block diagram of Figure 1, the basic servo system elements are an inertial load (the gimbal and detector), a torque motor, a torque amplifier,feedback and manual positioning potentiometers,and identical operational amplifiers and phase lead filters. An equivalent conventional servo diagram of this system without the phase lead filters is shown in Figure 4.

The torque motor and torque amplifier were selected on the basis of the detector moment of inertia and the maximum power that could be used to drive the motor. Given a specific load, motor and torque amplifier, the design problem is to determine the amplifier gain and a suitable compensating network (filter) to obtain the frequency response characteristics desired.

Two reasonable requirements for the gimballed detector servo system are:

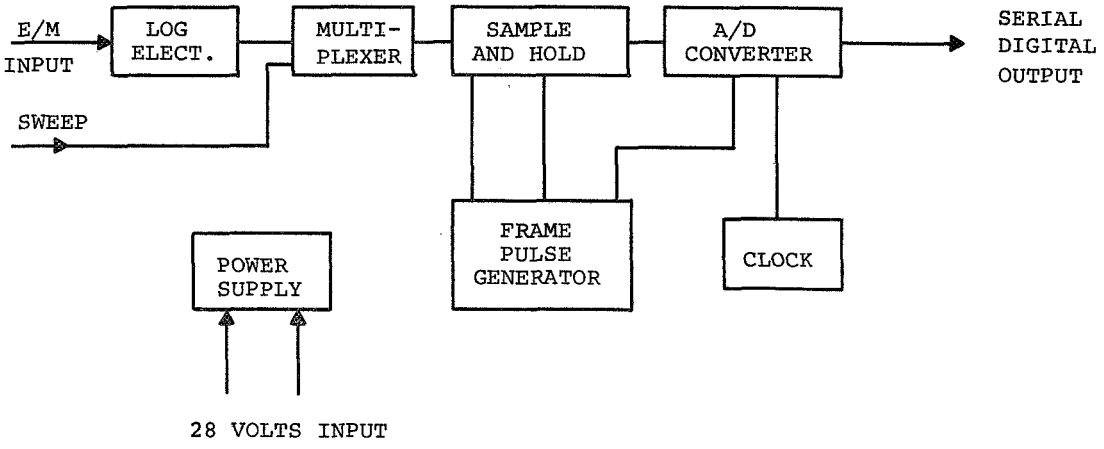

Figure 3. Block Diagram of Signal Processing Electronics.

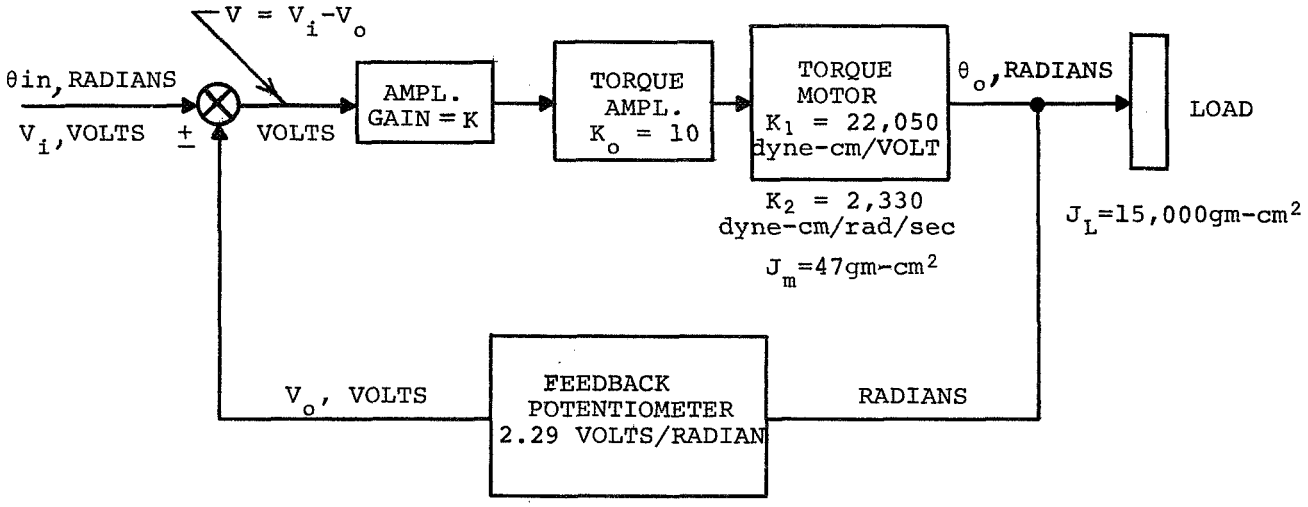

Figure 4. Equivalent Servo System Block Diagram.

(1) Frequency response to be flat to at least 3 degrees/sec (1/120 cycle/sec or 6.28/120 radians/sec).

(2) Servo to be slightly underdamped (a small amount of overshoot in the step response is desired).

The equation of motion for a motor driving a load can be developed as shown below: The output torque T of the motor varies directly with the input voltage and is decreased by a viscous drag torque caused by the back emf that is developed as a result of the motor speed. Using the symbols θ for angular rotation (in radians), t for time (in seconds), and V for input voltage to the motor (volts), one can write:

$$T = K_1 V - K_2 (d\theta/dt) \qquad (1)$$

where K_1 is the torque per unit input voltage in dyne-cm/volt.

The total moment of inertia J can be written as:

$$J = J_m + n^2 J_L \qquad (2)$$

where J_m is the moment of inertia of the motor rotor, J_L is the moment of inertia of the load, and n represents the gear ratio or ratio of the load speed to the motor speed. Moments of inertia are given in the units gm-cm^2.

According to Newton's Law for rotational motion, we have:

$$T = J(d^2\theta/dt^2) \qquad (3)$$

Substituting from equations (1) and (2) into (3) yields the equation of motion of the motor and load:

$$J(d^2\theta/dt^2) + K_2(d\theta/dt) = K_1V \qquad (4)$$

The above equation may be Laplace transformed to give the transfer function of the motor and load:

$$\frac{L(\theta)}{L(V)} = \frac{K_1}{Jp^2+K_2p} = \frac{K_1/K_2}{p\left[\frac{J}{K_2}\,p+1\right]} \qquad (5)$$

The values of the parameters K_1, K_2, and J are obtained from the motor manufacturer and the weight and dimensions of the gimballed detector. The following values apply:

$J_L = 15{,}000$ gm-cm^2

$J_m = 47$ gm-cm^2

$J = 15{,}047$ gm-cm^2

$K_1 = 2.205 \times 10^4$ dyne-cm/volt

$K_2 = 2.33 \times 10^3$ dyne-cm/rad/sec. Max.(zero source impedance)

$= 3.53 \times 10^1$ dyne-cm/rad/sec. Min. (infinite source impedance).

The transfer function of the motor and load then becomes

$$\frac{1}{P}\left[\frac{9.464}{6.44p+1}\right] \text{ radians/volt (zero source impedance)}$$

The servo diagram of Figure 4 now becomes the transfer function diagrams given in Figure 5.

In order to determine the stability, a plot of AB and A/(1 + AB) is needed. In this case, since B is a constant, 2.29 volts/radian, a Bode plot of AB/(1 + AB) can be used instead of A/(1 + AB).

Assume a value of K initially such that

$$K = \frac{1}{(2.29)\ (94.64)} = \frac{1}{216.7}$$

We then have the open loop transfer function:

$$AB = \frac{1}{p(6.44p+1)}$$

This transfer function is constructed graphically by use of Bode plots of 1/p and 1/(6.44p+1). From the graph of the magnitude and phase shift of AB, it is seen that the AB gain is 44 db below 0 db at a phase shift of -180 degrees so that the servo system is stable. The gain could be increased by 44 db (a factor of 158) and the system would still be stable.

Next AB is plotted on a Nichols Chart to determine the closed loop response.

From the closed loop frequency response curve, we find that the system resonant frequency f_r = 0.4 rad/sec equivolent to 0.0637 cps. The bandwidth is f_b = 0.6 rad/sec

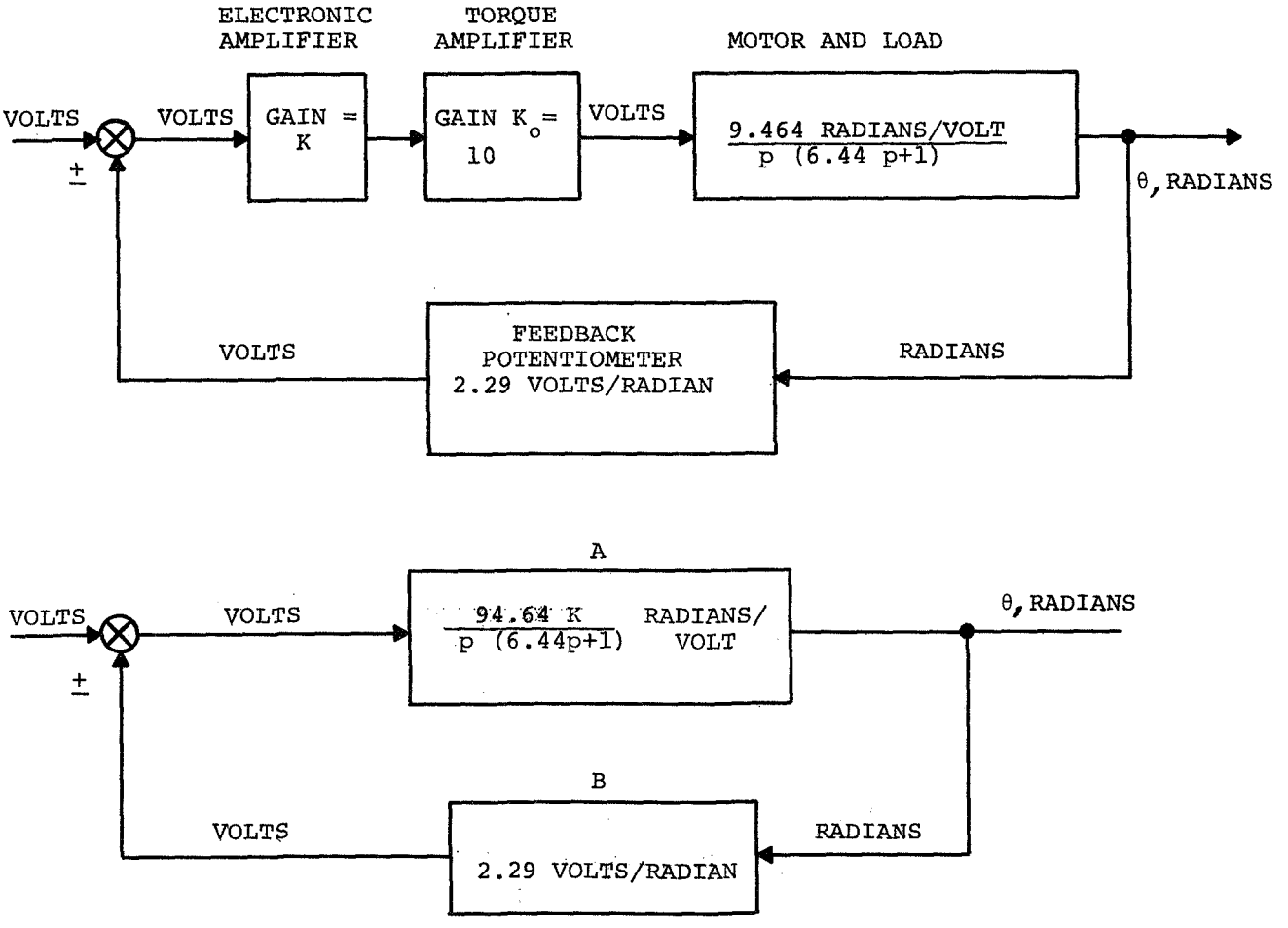

Figure 5. Transfer Function Diagrams.

equivalent to 0.0956 cps. The peak in the closed loop response is +8.5 db indicating strong underdamping. Increasing the gain of the amplifier would increase the frequency response but would decrease the damping.

In order to increase the frequency response and the damping, it is necessary to install a phase lead filter in the system. After several preliminary trials, a phase lead network of the form

$$\frac{\frac{1}{\omega_2}\,p+1}{\frac{1}{\omega_1}\,p+1} = \frac{5\,p+1}{0.5\,p+1}$$

was chosen.

The amplitude (in db) and the phase shift in degrees of the above filter transform function were plotted on the same Bode plot as the servo transform functions $1/p$ and $1/(6.44p+1)$. The magnitudes of the functions are added and their phases are added to give new magnitude and phase curves for the network-modified servo. After this was done, it became apparent that an additional gain of 11 db was needed to increase the overshoot to the desired value of +3 db.

The result of the lead network and an additional gain of 11 db was to make the theoretical frequency response flat out to 2.8 rad/sec = 0.44 cps. The system resonant frequency would be 2.0 rad/sec = 0.32 cps = f_r . The bandwidth would be f_b = 3.30 rad/sec = 0.526 cps (3 db down). The peaking M = 0.41.

The servo's theoretical response to a step input could be determined on the basis of the following well-known transformation between the frequency response curve (drawn with a linear scale instead of a db scale) and a linear step response curve. Referring to Figure 6, the relationships between the two curves are:

1. The transient overshoot A_1 is about 3/4 of the peaking M in the frequency response curve. A_1 cannot exceed 100 percent.

2. The transient rise time T_R (seconds) is related to the bandwidth f_b cps by the relationship:

$$T_R = 0.45/f_b$$

if A_1 = 10 percent or more.

3. The time to reach the peak value T_p, in seconds, is related to the resonant frequency f_r cps by:

$$T_p = 0.5/f_r$$

4. The ratio of successive undershoots and overshoots is approximately

$$\frac{1}{A_1} = \frac{A_1}{A_2} = \frac{A_2}{A_3} = \frac{A_3}{A_4} \quad \text{etc.}$$

5. The frequency of the ringing oscillation in the transient response is approximately equal to the system resonant frequency f_r.

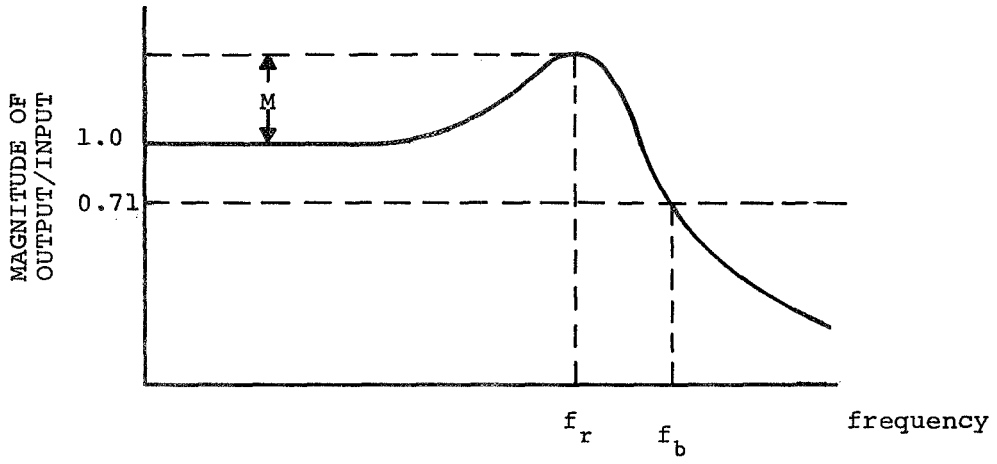

FREQUENCY RESPONSE

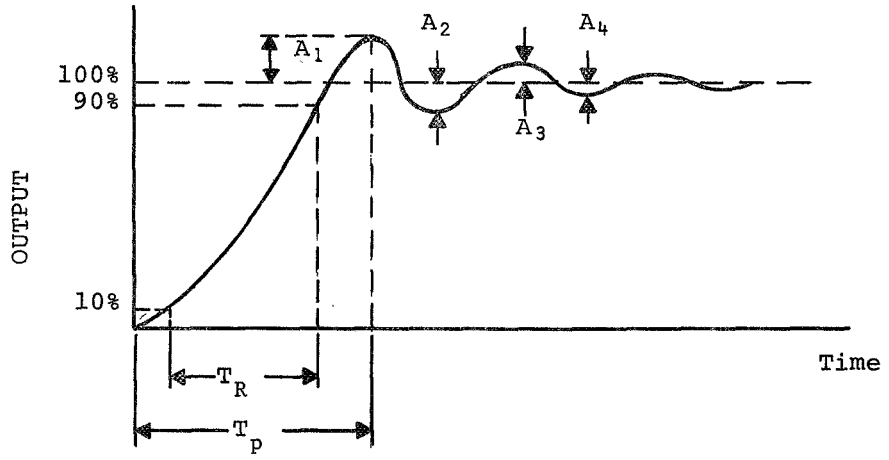

STEP RESPONSE

Figure 6. Equivalent Frequency Response and Step Response for a Typical Underdamped Servo.

Using the relationships listed above, one finds the following characteristics for the modified servo's response to a step input:

1. The transient overshoot $A_1 = .30$ or 30%.

2. The transient rise time $T_R = 0.855$ sec.

3. The time to reach peak value $T_p = 1.57$ sec.

4. The ratio of successive overshoots and undershoots = 3.3.

5. The frequency of the ringing oscillation $f_r = 0.32$ cps.

The lead network filter has the form shown in Figure 7. The transfer function for this network can be written as

$$\frac{5p+1}{0.5p+1} = \frac{10(5\times10^5 p+10^5)}{(5\times10^5 p+10^6)} = \frac{10(R_1R_2C)p+R_2}{(R_1R_2C)p+(R_1+R_2)}$$

Ignoring the factor of 10 for the moment, one can solve to find the values of R_1, R_2, and C:

$$R_1 = 900K\ , \quad R_2 = 100K\ , \quad C = 5.56\mu_f$$

The amplifier gain K was initially assumed to be $K = 1/216.7$. Due to the filter loss, this gain must be increased by a factor of 10. It must also be increased by 11 db (a factor of 3.55) to obtain the desired response. Theoretically, the total gain of the amplifier should then be

$$K = \frac{1}{216.7} \times 10 \times 3.55 = 0.164\ .$$

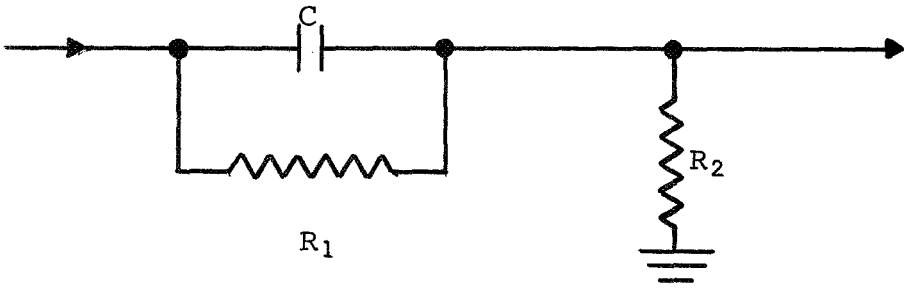

GENERAL FORM: $$\frac{T_1 p + K_1}{T_2 p + K_2}$$

EXACT FORM: $$\frac{(R_1 R_2 C)p + R_2}{(R_1 R_2 C)p + (R_1 + R_2)}$$

Figure 7. Lead Network Filter.

The amplifier gain is less than unity, indicating the need for attenuation, which can be obtained with a simple resistive divider.

In order to check the approximate design described above, a root-locus study was made of the subject servo system. Such a study permitted the system to be redesigned in an optimum fashion.

The transfer function block diagrams of Figure 4 can be transformed to a unity feedback diagram as shown in Figure 8.

Using the standard notation for the transfer function, one can write:

$$KG = K\frac{N}{D} = \frac{33.6Q}{p(p+.155)}$$

so that $N = 1$, $K = 33.6Q$ and $D = p(p+.155) = p^2+.155p$. The root-locus can then be drawn for this servo. There are two finite poles at $p = 0$ and $p = -.155$, and there are no finite zeroes. There will be a root-loci to the left of the pole at $p = 0$ (an odd number of poles). Since the root-loci end on zeroes, there will be two zeroes at infinity. These zeroes will lie on asymptotes that intersect at

$$q_1 = \frac{d_1+d_2+d_3+\ldots - (n_1+n_2+\ldots)}{m}$$

$$= \frac{-.155-0}{2} = -.0775$$

where d_1, d_2, etc. are the coordinates of the finite poles of G and n, n_2, etc. are coordinates of the finite zeroes of G. Here m is the number of zeroes at infinity.

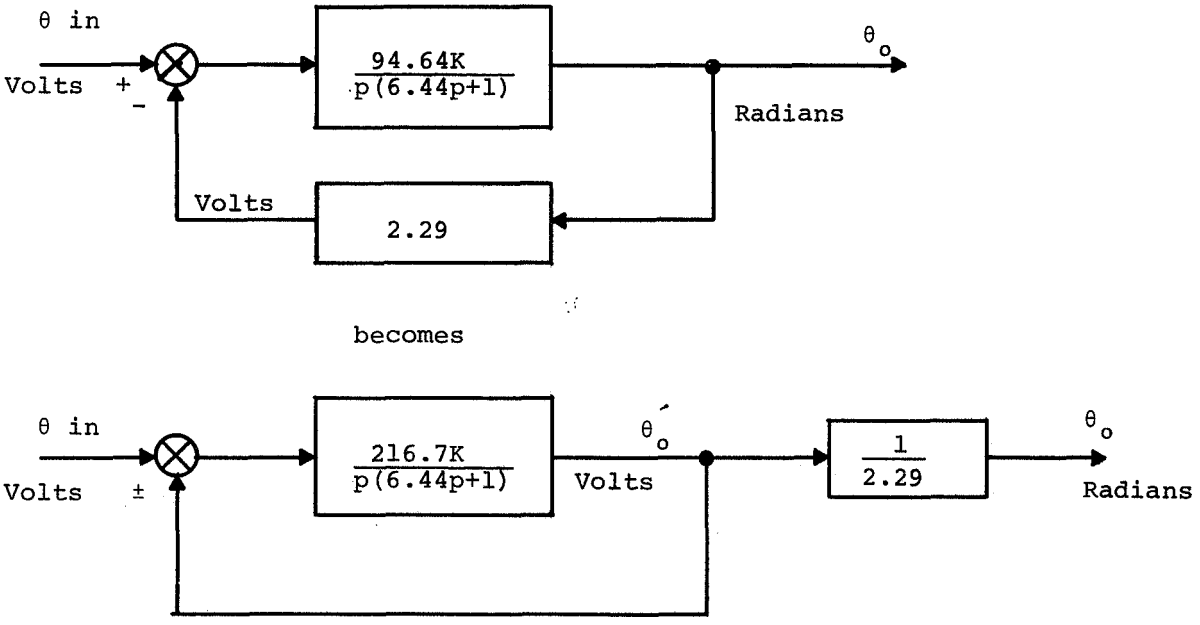

or, letting Q be the variable gain of the amplifier instead of K:

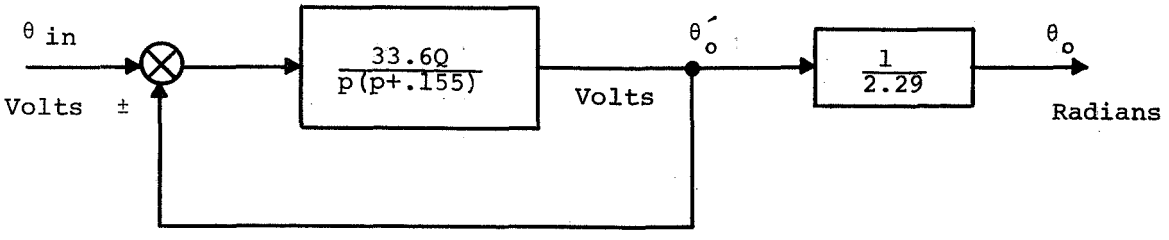

Figure 8. Unity Feedback Transfer Function Diagrams.

The breakaway point between $p = 0$ and $p = -.155$ is located at $b = -.0775$ since at a breakaway point the sum of the reciprocals of the distances from the poles and zeroes is zero, and breakaway points always appear to the left of an odd number of poles or zeroes.

Since there can be no roots to the right of $p = -.0775$, the servo will always be stable independent of the gain. However, the servo damping will vary with the gain.

If the frequency response is to be flat to 1 cps, this implies a step response transient rise time from 10 to 90 percent of final value of about

$$T_R = \frac{0.45}{1} = 0.45 \text{ seconds.}$$

The significant time constant must be less than T_R in order to meet this requirement, so that all roots would have to be farther to the left than

$$p = \frac{-1}{0.45} = -2.22$$

Hence let us shift the pole from $p = -.155$ to $p = -4$. This is done by inserting a pole at $p = -4$ and a zero at $p = -.155$. The filter that accomplishes the above has a transfer function:

$$\frac{p + .155}{p + 4}$$

Multiplying the above transfer function with the transfer function appearing in Figure 8 yields the new transfer function for the redesigned servo:

$$KG = \frac{33.6Q}{p\ (p+4)}$$

where

$$N = 1$$

$$K = 33.6Q$$

$$D = p\ (p+4) = p^2 + 4p$$

$$D + KN = p^2 + 4p + 33.6Q$$

The asymptotes now intersect at $q_1 = -2$, and the break-away point at b must also be at $b = -2$.

In order to find a proper operating point on the root locus, one draws two straight lines on the root locus plot that start at the origin and make angles of plus and minus 70° with respect to the negative real axis. These lines will intersect the root loci at roots that correspond to a damping coefficient of .342 (cosine of 70°), typical of an underdamped servo. Assuming that the loci are close to the asymptotes, the intersections with the asymptotes are found graphically to be $r_1 = -2 + j\ 5.5$ and $r_2 = -2 - j\ 5.5$.

The value of K that corresponds to the roots r_1 and r_2 is obtained by direct measurement of the distances (graphically) from the root to the poles according to the equation:

$$K = \frac{(\overline{p_1 - d_1})\ (\overline{p_1 - d_2})\ (\overline{p_1 - d_3})}{(\overline{p_1 - n_1})\ (\overline{p_1 - n_2})}$$

Since there are no zeroes n in this system, only the distances between each root and the poles contributes to K. It is found graphically that

$$K = (5.85)\ (5.85) = 34.3$$

Since $K = 33.6Q$, $Q = 34.3/33.6 = 1.02$.

The filter (compensating network) design can be written as:

$$\frac{p + .155}{p + 4} = \frac{10^5\ p + .155\ (10^5)}{10^5\ p + 4 \times 10^5}$$

Using the same form of resistor capacitor network as before, it is found that $R_1 = 384.5K$, $R_2 = 15.5K$ and $C = 16.8\mu f$.

The closed loop frequency response of the redesigned servo is found by first calculating the ratio of $\theta o'$ (intermediate output) to θ_{in} (input) for a series of frequencies ω from the expression:

$$\frac{\theta o'}{\theta_{in}}\ (\text{magnitude}) = \frac{K}{\ell_1 \ell_2}$$

where ℓ_1 and ℓ_2 are the distances measured from the two roots r_1 and r_2 to a point $p = j\omega$ on the imaginary axis. The value obtained for $\theta o'/\theta_{in}$ is thus a function of the frequency ω. The final ratio of $\theta o/\theta_{in}$ for each frequency ω

is obtained by multiplying the intermediate ratios $\theta o'/\theta_{in}$ by the factor 1/2.29 radians/volt. The resulting magnitude ratios can then be expressed in db and plotted as shown in Figure 9.

From the frequency response curve, the following information pertaining to this theoretical servo can be obtained:

1. The frequency response is flat out to 7.3 radians/sec or 1.2 cps.

2. The system resonant frequency is 5.5 rad/sec = 0.88 cps = f_r.

3. The bandwidth is 8.4 rad/sec = 1.3 cps = f_b.

4. The peaking M = 0.55 (estimated).

The servo's approximate response to a step input should be:

1. The transient overshoot is (3/4)M = 41%.

2. The transient rise time is $0.45/f_b$ = 0.35 sec = T_R.

3. The time to reach peak value is $0.50/f_r$ = .57 sec = T_p.

4. The ratio of successive undershoots and overshoots is

$$\frac{1}{A_1} = \frac{1}{.41} = \frac{A_1}{A_2} = \frac{A_2}{A_3} = 2.4$$

5. The frequency of the ringing oscillation is 0.88 cps = f_r.

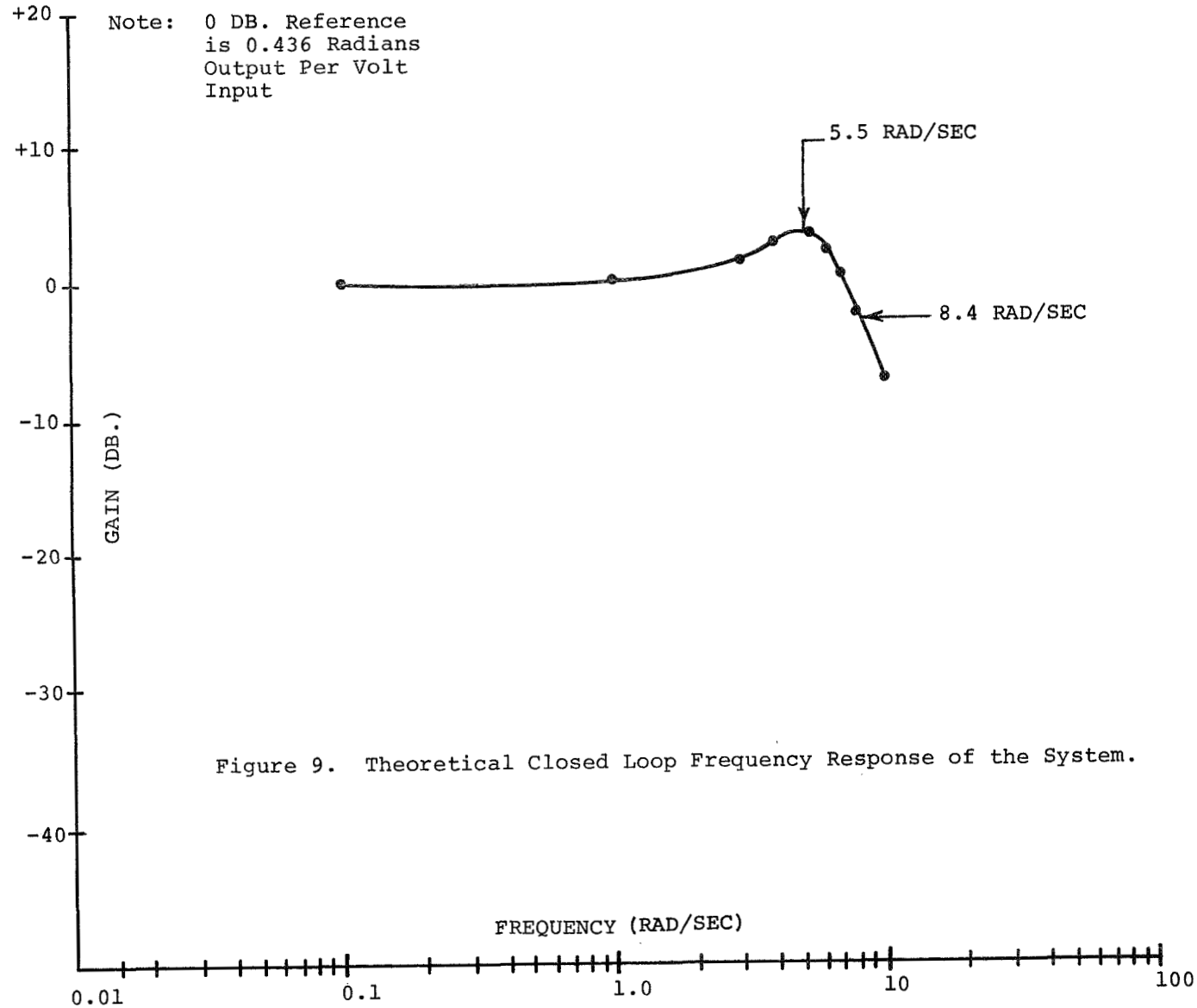

Figure 9. Theoretical Closed Loop Frequency Response of the System.

The transient response for a step input function of 2 volts, for example, can also be derived directly from the transfer function as follows:

$$\theta_o' = \frac{K}{(p-r_1)(p-r_2)} \left[\frac{2}{p-0}\right] = \frac{34.3}{[p-(-2+j5.5)][p-(2-j5.5)]} \frac{2}{(p-0)}$$

$$\theta_o' = Br_o e^{ot} + Br_1 e^{+r_1 t} + Br_2 e^{+r_2 t}$$

where

Br_o = the residue of θ_o' at $p = 0$

Br_1 = the residue of θ_o' at $p = r_1$

Br_2 = the residue of θ_o' at $p = r_2$

Evaluating Br_o, Br_1 and Br_2, one obtains:

$$\theta_o' = 2.00 + .730\ e^{-2t} \sin 5.5t - 2.00\ e^{-2t} \cos 5.5t = 2.29\theta_o$$

so that

$$\theta_o' = 0.875 + .319\ e^{-2t} \sin 5.5t - .874e^{-2t} \cos 5.5t \text{ radians.}$$

The displacement θ_o is plotted as a function of time in Figure 10.

Note: .874 Radians
$\cong 50°$

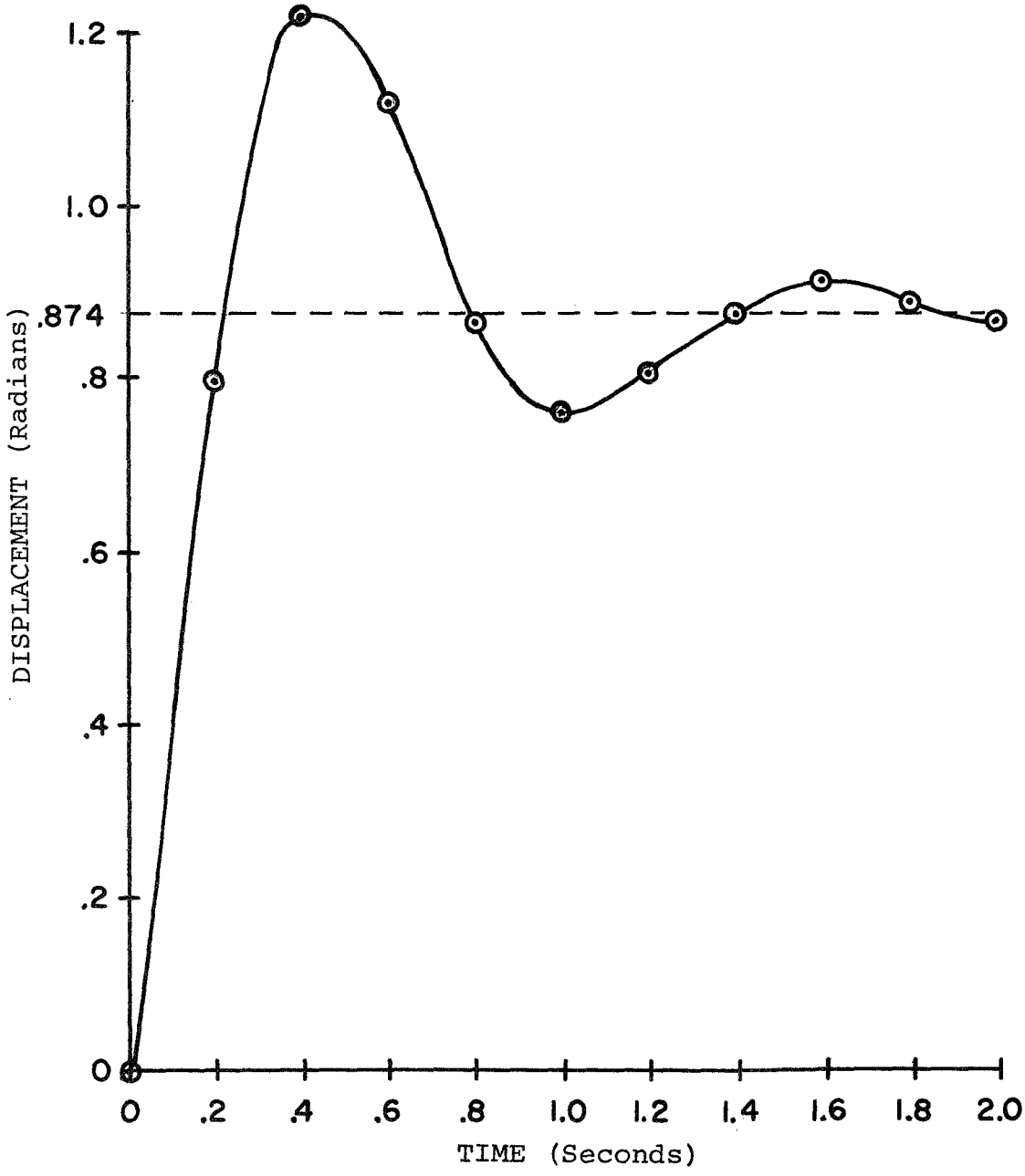

Figure 10. Theoretical Servo Response to a 2 Volt Step Input.

The theory of generalized error constants may also be used to determine the response of a servo to a suddenly applied transient such as a step, ramp or parabolic input. The laplace transform of the ratio of error signal to input signal may be written as:

$$\frac{E}{I} = \frac{1}{1+K_p} + \frac{P}{K_v} + \frac{p^2}{K_a} + \frac{p^3}{K_j} + \ldots$$

where K_p is the position error constant, K_v is the velocity error constant, K_a is the acceleration error constant, and K_j is the jerk error constant. The error constants can be found by expanding E/I in a Maclaurin's series of the form:

$$F = F_o + F_1\, p + F_2\, \frac{p^2}{2.1} + F_3\, \frac{p^3}{3.2.1} + F_4\, \frac{p^4}{4.3.2.1} + \ldots$$

where F_o = the value of F at $p = 0$, F_1 = the value of dF/dp at $p = 0$, F_2 = the value of d^2F/dp^2 at $p = 0$, etc.

For our servo, we have:

$$\frac{E}{I} = \frac{1}{1+AB} = \frac{1}{1+\frac{34.3}{p(p+4)}} = \frac{p(p+4)}{p(p+4)+34.3}$$

and $$F_o = \left.\frac{E}{I}\right|_{p \to 0} = 0 \quad \text{so that} \quad K_p = \infty$$

$$F_1 = \left.\frac{d}{dp}\left(\frac{E}{I}\right)\right|_{p \to 0} = \frac{4}{34.3} \quad \text{so that} \quad K_v = \frac{34.3}{4} = 8.58$$

and

$$F_2 = \frac{d^2}{dp^2}\left(\frac{E}{I}\right)\Bigg|_{p \to 0} = \frac{18.3}{40{,}400} \text{ so that } K_a = \frac{40{,}400}{18.3} = 2200.$$

The actual error (before the attenuator 1/2.29) is

$$\varepsilon = \left[\frac{1}{1+K_p}\right] i + \frac{1}{K_v}\frac{di}{dt} + \frac{1}{K_a}\frac{d^2i}{dt^2} + \ldots$$

One can then find the error for any given input function i(t). For example, if the input function is $i = \frac{1}{3}t^2$, so that there is a uniform acceleration with time, one finds that at the end of 3 seconds

$$i = 3, \quad \frac{di}{dt} = 2 \quad \text{and} \quad \frac{d^2i}{dt^2} = \frac{2}{3}, \text{ so that for our servo,}$$

$$\varepsilon = \frac{3}{1+\infty} + \frac{2}{8.58} + \frac{2/3}{2200} + \ldots \cong .23.$$

Both the output and the error are reduced by a factor of 2.29.

The steady state error can be determined from the dynamic error constants. For example, the time for the system to recover half-way from a sudden disturbance (step input) is approximately $1/K_v$ sec (equal to 0.117 seconds for our servo). The steady state displacement error for a step input of A radians is A/K_p (equal to zero for our servo). The steady

state error for a velocity ramp input is ω/K_v where ω is the rate of rise of the ramp in output units per second (equal to 0.117 ω radians for our servo). The time for the servo output to half-way complete the transition from rest to full speed is again approximately $1/K_v$ seconds (equal to 0.117 seconds for our servo). Again as an example, if the ramp input changes at a rate of ω = 3°/sec, the steady state error (lag) will be (.052 radians/sec)(0.117) = 0.0061 radians ≅ 24 minutes.

The moment of inertia calculation for the servo system was made on the basis of a typical, small miniquadrupole mass spectrometer that had been constructed. This quadrupole consisted of four major masses: 1) Source and Magnet, 2) Quadrupole rods and associated elements, 3) Electron multiplier and connectors and 4) Case. In addition to these basic detector elements, one must add a static balancing mass and the detector head mass.

If each of the six elements listed above is first considered as a point mass, the total moment of inertia I would be:

$$I = \sum_i I_i = \sum_i m_i r_i^2$$

where the m_i are the masses of these elements and the r_i are their distances from the pivot point. The moment of inertia of these point masses was calculated to be 9,587 gm cm^2. In addition to the above, one must include the moment of inertia of each element or component about its own center of mass. The result of the latter calculation yielded a moment of 3,686 gm-cm^2. According to the parallel axis theorem, the

total moment of inertia is the sum of the two moments calculated, or a total of 13,272 gm-cm^2. To the above moment of inertia one must add the moment of inertia of the detector trunnion assembly and the detector clamp, as well as that of the gimbal for yaw motions. For servo calculation purposes, it was assumed that the Load (detector) moment of inertia was 15,000 gm-cm^2.

In order to test the gimballed detector system, it was necessary to design a simulated quadrupole mass spectrometer (detector). The design goal was a total moment of inertia of 15,000 gm-cm^2. The simulated mass spectrometer was designed by first assuming a basically simple configuration and then modifying the mass distribution to obtain the desired total mass of 360 grams and moment of inertia of 15,000 gm-cm^2.

The basic configuration chosen for the simulated detector was a solid cylinder of aluminum 0.750 inches in diameter and 9.000 inches long. This cylinder was then modified in two ways: first by providing two sections of larger diameter (1.313 inch diamter) in the vicinity of the pivot point and at the front end where the detector head would be attached, and second, by providing counterbores at both the front end and the back end, each having a different depth.

By using a technique of successive approximations, a simulated detector was designed which was only 5.3 grams overweight (about 2 percent overweight) and had a moment of inertia of 15,405 gm-cm^2, about 3 percent greater than the design value. The design could obviously be refined to more closely approximate the parameter design values, but this refinement was believed to be unnecessary in view of the uncertainty of the original assumption concerning the total moment of inertia.

The residual error between the desired and the actual position of the gimbal in this servo system is determined by either the resolution of the feedback potentiometer or the static friction of the potentiometer and bearings.

Since the feedback potentiometer furnishes 1000 ohms for 352 degrees of rotation or 0.352 degrees/ohm, and since the potentiometer minimum resistance increment is 1.52 ohms, the minimum angle increment will be 0.53 degrees if the servo system can follow this incremental change in feedback resistance (actually the equivalent feedback voltage).

The feedback potentiometer will be adjusted to provide 2.29 volts per radian of rotation of the gimbal as discussed earlier. If one multiplies this quantity by .01745 radians/degree, the result is 0.040 volts/degree at the input of the torque amplifier. The torque amplifier gain is fixed at 10, so the amplifier output voltage per degree of misalignment between output gimbal and input will be 0.40 volts. The resistance of the torque motor is 48 ohms, so that a voltage of 0.40 volts will produce a motor current of 0.40/48 = .00834 ampere/degree. Since the sensitivity of the torque motor is 15 oz-in./ampere a one degree misalignment will generate an initial driving torque of .125 oz-in., which may not quite overcome the maximum static friction of 0.15 oz-in. of the potentiometer. In fact, the misalignment will have to be at least 1.20 degrees in order to generate a torque of 0.15 oz-in.. The accuracy with which the gimballed detector will reproduce a desired position will then be ± 1.20 degrees. The accuracy will be improved if the potentiometer static friction is reduced or if the feedback signal is increased.

The design parameters for the digital output signal processing electronics include the following requirements: (1) Two analog signal (0 - 5 VDC) inputs, (2) Data rate high enough to reasonably reconstruct the mass peaks with a sweep rate of 5/sec, (3) Ten bit data word format, (4) Minimum weight, and (5) Minimum power derived from a 28 VDC source. The block diagram of Figure 3 will help in understanding the electronics.

Item (1) will require multiplexing the two signals to provide alternate digital data points using a single analog to digital (A/D) converter. The multiplexer is essentially a pair of switches which route the incoming signals alternately through a sample and hold circuit to the A/D converter. The sample and hold is necessary to maintain a constant data point for the A/D converter.

Item (2) is calculated from the sweep rate, 5/sec, or for 0 - 50 AMU mass range, 250 peaks per second, and, assuming 10 data points per peak, 2500 data points per second. Because two signals are multiplexed, the A/D converter must handle 5000 data points per second. With a ten bit word (Item 3) per data point, the basic bit rate will be 50 KHz, which is a reasonable speed for a successive approximation analog to digital converter.

The A/D converter operates by comparing an internally generated reference voltage with the analog input and successively stepping the reference by factors of ½ (for binary coding) up or down, as required, to approach the value of the incoming signal. For the first or most significant bit (MSB), the comparison is ½ of the total range (0 - 5 VDC) or 2.5 volts. If the analog input is greater than 2.5 V the first bit is a "1", if less, the first bit is "0". The second bit is determined by the comparison

of the analog voltage to 3.75 volts if the first bit is "1" (greater than 2.5 volts) or 1.25 volts if the first bit is "0" (less than 2.5 volts). Succeeding bits are similarly formed by comparison with the voltage representing the previous bits plus ½ the remainder. The output is then a time succession of "1" s or "0" s. At the end of each ten bit conversion, the multiplexer is stepped to the alternate input and a new conversion is performed.

DESIGN AND CONSTRUCTION

Mechanical Elements

Following the theoretical study of the servomechanical elements of the gimballed detector system, design of a prototype system was started. It was realized at the outset that the gimballed detector servo system could be constructed in the following different forms:

a) An ac, 400 cps servo system using 2-phase motors.

b) A dc servo system using a geared-down dc motor.

c) A dc brushless, limited angle, direct drive servomotor system.

It was decided that an ac system was not practical since the primary power available on most rockets is direct current. It would take a great deal of power and weight to generate the 115 volts 400 cycles usually used for such servo systems. Other drawbacks would be the necessity for gear reduction of motor speeds and transmission of motion through a vacuum wall. If the drive motors were placed inside the vacuum enclosure, there would be problems with component placement and outgassing.

In ac servosystems, there is usually a continuous dissipation of power in a fixed field phase.

A dc servo system using a high speed, geared-down dc motor has many of the same disadvantages as a geared-down ac motor system. In addition, the sparking and noise generated by the commutator of a dc motor can interfere with other equipment. The operation of such a motor in a vacuum environment would require the use of special solid film lubrication for the commutator. In general, however, a brush type dc torquer does provide the most torque for a given size and weight, provides peak torque at any rotor position and furnishes a constant torque at constant velocities for an unlimited range of angular position.

A dc brushless, limited angle, direct drive servomotor system has advantages of simplicity, small size and weight, no gears with attendant backlash, friction, lubrication and outgassing problems and low power requirements. Since there are no brushes, there are no problems with friction, wear, sparking and noise. In addition, there is no ripple torque of the type experienced with dc brush type motors. It was decided that dc brushless, limited angle, direct drive servomotors were especially well suited to the application at hand. Such motors had been developed for use in vacuum environments and were commercially available together with matching differential input torque amplifiers (current amplifiers).

Having decided on the type of servomotor to use, the next step was to determine the type of feedback elements that would be best. In order to keep the system as simple as possible, it was decided to first try precision wire wound potentiometers as the feedback elements. Potentiometers can be used with dc voltages whereas ac voltages are required by synchro repeaters.

Potentiometers can be made with low friction torques of the order of 0.15 oz-in. These potentiometers can be dry-film lubricated for vacuum service (although this was not actually done in our development work). Potentiometers provide a direct indication of gimbal position and require a minimum of electrical connections.

The method of preserving the vacuum integrity of the detector housing while permitting motion of the detector is a key element of the design. Initial designs called for the use of metal bellows at the front of the instrument. Metal bellows, even of the flexible welded variety, require a great deal of force or torque to move them. These bellows are quite heavy and bulky and would restrict the angular motion of the detector.

It was decided to use a spherical gap, low vacuum conductance seal at the front of the detector housing. Such a vacuum seal, while not perfect, would allow only a negligible amount of external ambient gas to enter the detector housing during flight operation while permitting the detector to be moved freely without any friction whatsoever. Figure 2 shows the spherical gap low conductance seal arrangement.

The detector (quadrupole mass spectrometer) would be housed in a cylindrical case about 6½ inches in diameter and 13 inches long. Plate glass windows would be temporarily installed at the front and rear of the case so that the gimbal motion could be observed. The case and windows would be fastened together with Torr Seal epoxy plastic so that they could be easily disassembled.

The gimbal system, spherical gap housing head and cylindrical case would be made primarily of 6061 T-6 aluminum to obtain high strength with low weight. Some components of the

gimbal (bearing surfaces, for example) would be made of 304 stainless steel. It was decided to provide a heavier gimbal in the initial design to allow for later lightening, modifications and changes.

The bearings used with the gimbal system had to be capable of operating in a vacuum environment. For this reason, Barden Corp. "Bartemp" ball bearings were specified since these bearings contain elements (ball separators) that provide molybdenum disulphide as a dry lubricant for vacuum service.

Having decided on the principal components of the gimballed detector, the next step was to design the gimbal itself. The moveable gimbal, a rectangular, open, box-like structure, is mounted in bearings within the gimbal mount. The gimbal mount is a one-piece structure containing sections of a cylindrical ring to center it within the cylindrical detector housing or case. Other portions of the gimbal mount provide flat mounting surfaces for the torque motors and feedback potentiometers. The gimbal, torque motors, feedback potentiometers and detector trunnion assembly are shown in the gimballed detector mount assembly sketch of Figure 11. The detector is friction clamped within the trunnion assembly.

Electrical connections to the two torque motors and the two feedback potentiometers are brought into the case via an hermetically sealed electrical connector located near the rear of the case. Moveable elements such as the gimbal torque motor and feedback potentiometer are connection electrically with small diameter, coiled, enamelled magnet wires that offer a minimum of resistance to movement.

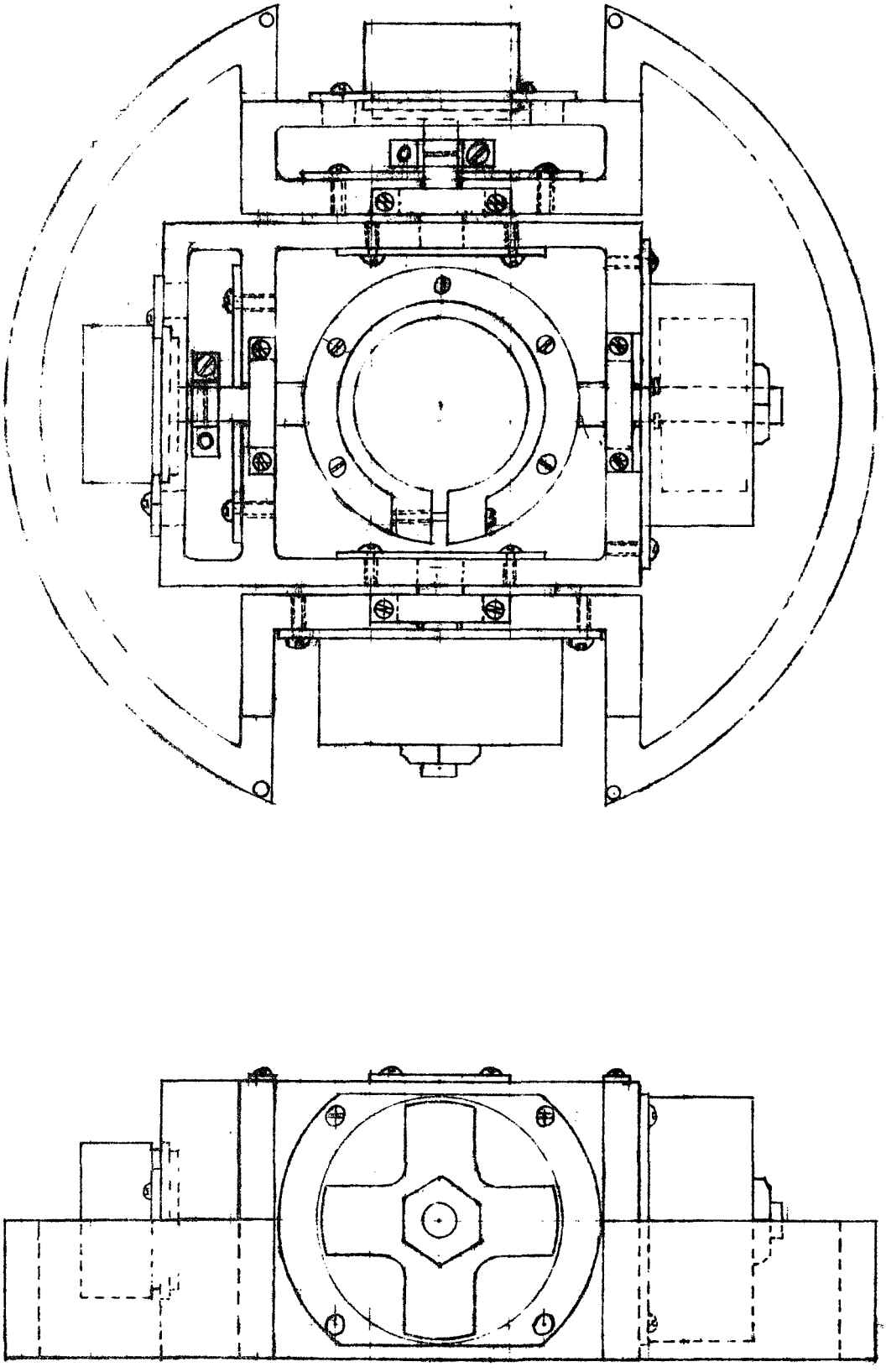

Figure 11. Gimballed Detector Mount Assembly.

Sketches were prepared of each of the individual mechanical components including a specialized wrench that would be required for assembly. Sketches were used instead of formal drawings to save time, minimize the cost and allow changes to be made easily.

The greatest effort went into the design of the gimbal and the gimbal mount. Tolerances as small as .0005 inch were specified for critical bearing retainer holes and counterbores. The 6061 T-6 Aluminum used for the gimbal, the gimbal mount, the spherical detector head, the spherical housing head and the housing cylinder was stress relieved before critical finish machining. All important surfaces, including internal surfaces of the vacuum housing, were machined to a 32 finish. All edges were broken.

Looking more closely at individual mechanical components, the gimbal was machined out of a solid piece of aluminum 2 inches thick. Concentric holes were drilled for the pitch bearings and potentiometer. The gimbal was designed so that the detector trunnion assembly together with its mounted pitch ball bearings could be lowered through slots into a final position at the center of the gimbal. The pitch bearings were locked into position by means of bearing retainer slides that filled the gimbal slots. Stainless steel shafts were designed to fasten to the gimbal on a line normal to the pitch bearing axis. These shafts would hold the yaw ball bearings.

The gimbal mount was also machined from a single piece of solid aluminum 2 inches thick. Again, concentric holes were drilled in this piece to hold the yaw bearings and potentiometer. As before, the gimbal mount was designed so that the entire gimbal together with its mounted yaw ball bearings could be lowered through slots into a final position at the center of the gimbal mount. The yaw bearings were locked into position by bearing retainer slides as before.

In the case of both the trunnion assembly and the gimbal, the stainless steel shafts which held the ball bearings were extended so that either a torque motor or a potentiometer could be mounted or coupled to each shaft. Torque motor rotors were mounted directly to their respective shafts via a threaded nut arrangement. The stators of these torque motors were mounted separately to the flat surfaces that held the ball bearings and were adjusted in position to provide a uniform clearance between the rotor and stator. The feedback potentiometers were mounted separate from, but concentric with, the trunnion and gimbal shafts. The latter shafts were coupled to the potentiometer shafts with the use of balanced gear clamps.

The gimbal, together with the pitch motor and potentiometer extensions, had sufficient clearance so that it could rotate inside the gimbal mount. Four mounting holes were drilled through the periphery of the gimbal mount to mate with drilled and tapped mounting holes in the housing head. The housing cylinder was made just large enough to slip over the gimbal mount.

The pitch and yaw axes intersected at the center of the gimbal mount, a point which shall be called the central pivot point. The housing head contained a spherical concave surface with its center at the central pivot point and a radius of 3.005 inches. The detector (a simulated detector was used in this project) was clamped in the trunnion assembly and fitted with a spherically convex detector head having a radius of 3.000 inches. The detector was positioned so that the center of the spherical detector head coincided with the central pivot point. In this way, a gap of .005 inch was created between the two spherical surfaces.

Both the housing head and the housing cylinder contained weld relief grooves so that a final permanent assembly of these two units might be made by heliarc welding. Similarly, the housing cylinder and housing cover were designed to be welded together for a final assembly. For experimental purposes, however, it was found that vacuum service epoxy such as Torr Seal held the components together in a vacuum tight fashion. The housing head and housing cylinder were held together mechanically with the use of special housing cylinder clamps before the Torr Seal was applied. The Torr Seal could be easily removed with any one of several recommended solvents. The hermetically sealed electrical connector was also fastened to the connector mount with Torr Seal, and the connector mount was fastened to the housing cylinder with Torr Seal.

In order to be able to watch the motion of the gimballed detector within the vacuum enclosure of the housing, a special top view cap and a special bottom view cap were designed and constructed. Each of these caps contained a counterbore 6 inches in diameter and ½ inch deep into which pyrex glass sight ports or windows were cemented with Torr Seal. The top view cap contained a ¼ inch I.D. pumping tubulation that could be used to evacuate the housing. The bottom view cap would be cemented within the back end counterbore of the housing cylinder.

The simulated detector was machined from a solid rod of aluminum. As indicated earlier, it was designed to have the same O.D. and length as an existing quadrupole mass spectrometer and still provide the correct weight, moment of inertia and balance.

The spherical detector head was fastened to the end of the simulated detector with a set screw. The detector was clamped

within the trunnion assembly so that the spherical detector head surface was just 3.000 inches from the central pivot point as explained earlier.

With the simulated detector aligned along the zero pitch-zero yaw axis (the longitudinal axis of the housing), the torque motors were adjusted to their zero positions and the feedback potentiometers were adjusted to their center positions.

Photographs of the gimballed detector mechanical components are shown in Figure 12. Here one can see the simulated detector mounted within the gimbal with the gimbal mount fastened to the housing head, as well as an exploded view showing the gimbal, gimbal mount, detector head and housing head separately.

Servo Control Unit

The control unit for the gimballed detector is basically very simple. Commercially available differential torque amplifiers provide a relatively large current (up to about 0.4 ampere) to drive the brushless torque motors. The torque amplifiers require +28 Volts dc input power and have a fixed voltage gain of ten. The feedback potentiometers are connected so as to modulate a dc signal voltage provided by separate dc power supplies in order to avoid coupling and cross talk between yaw and pitch motions.

Input filters or phase lead networks are provided at the inputs of the differential amplifiers to improve the system response. Operational amplifier circuits are used to isolate the relatively low torque amplifier input impedances from the filters. Various potentiometers are provided to adjust the sensitivity of the manual signal channels and the feedback channels. Switches are provided to change from manual to automatic operation on either yaw or pitch. Yaw and pitch circuits can be turned on and operated independently. The same

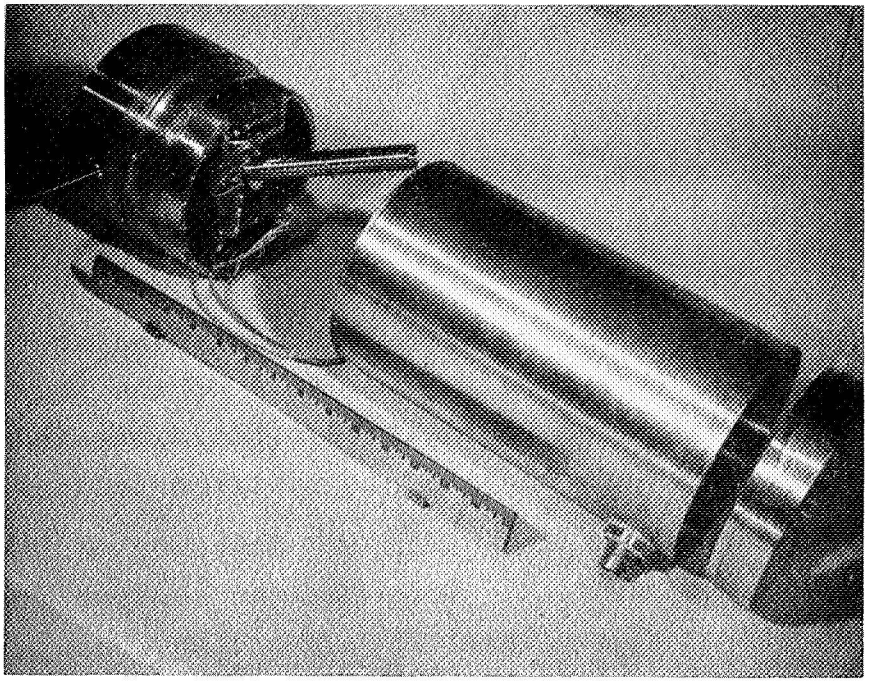

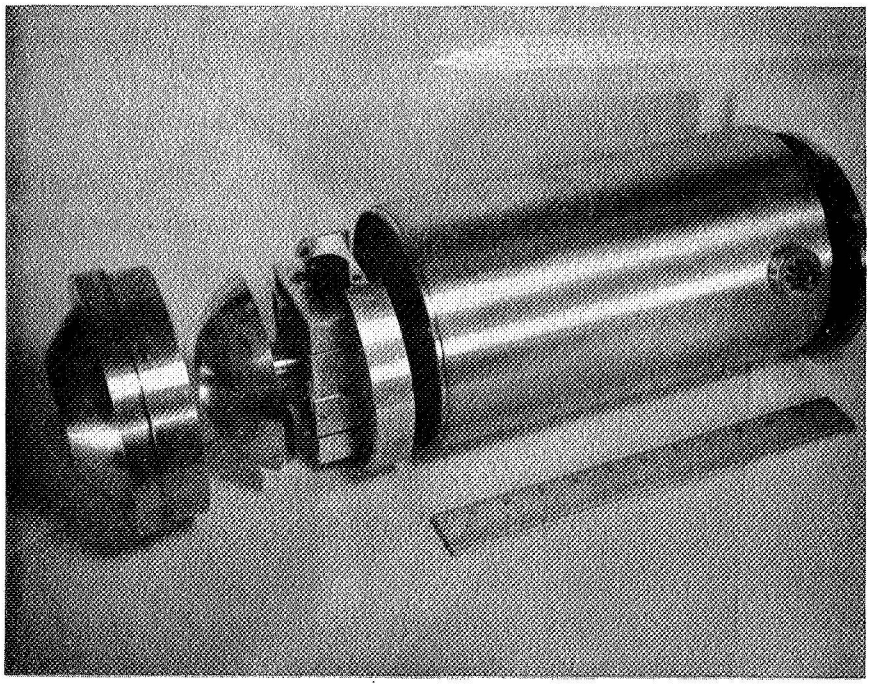

Figure 12. - Photographs of Gimballed Detector Mechanical Components.

type of precision wire wound potentiometers are used for the manual positioning as are used for the feedback potentiometers. A schematic of the control unit circuits is given in Figure 13.

A sloping panel cabinet was chosen to hold the control unit components. The manual pitch and yaw potentiometers are mounted on the sloping panel for ease of operation. Vernier dials graduated in degrees show the settings of the manual control potentiometers. Connections from the control unit to the feedback potentiometers and torque motors in the vacuum tight cylindrical case are made via octal plug connectors at the rear of the control unit and an electrical cable containing 11 leads.

Aeroflex Laboratories, Inc. brushless, wide angle dc torque motors, model TQ 18-7FC, were used to drive the gimbal assembly. Aeroflex Model TA-6DC all silicon transistor dc torque amplifiers were used to provide power to the torque motors. These amplifiers have a fixed voltage gain of 10 and a maximum power output of 6 watts. They require a single power input of 28 VDC and operate over the temperature range from - 50°C to +100°C. The amplifiers measure 3.19 x 2.69 x 0.80 inches and weigh 6 oz each. They have a frequency response that is flat to beyond 1000 hz. The input impedance is 10K from each of the differential input terminals to ground and the maximum output voltage is 20 volts. The amplifiers have output current limiting and short circuit protection.

The manual control potentiometers (and the feedback potentiometers) were Beckman Model 5203 R1K Single-Turn wirewound high temperature precision potentiometers. These units are linear to within ± 0.5 percent. They have a power rating of 2 watts at

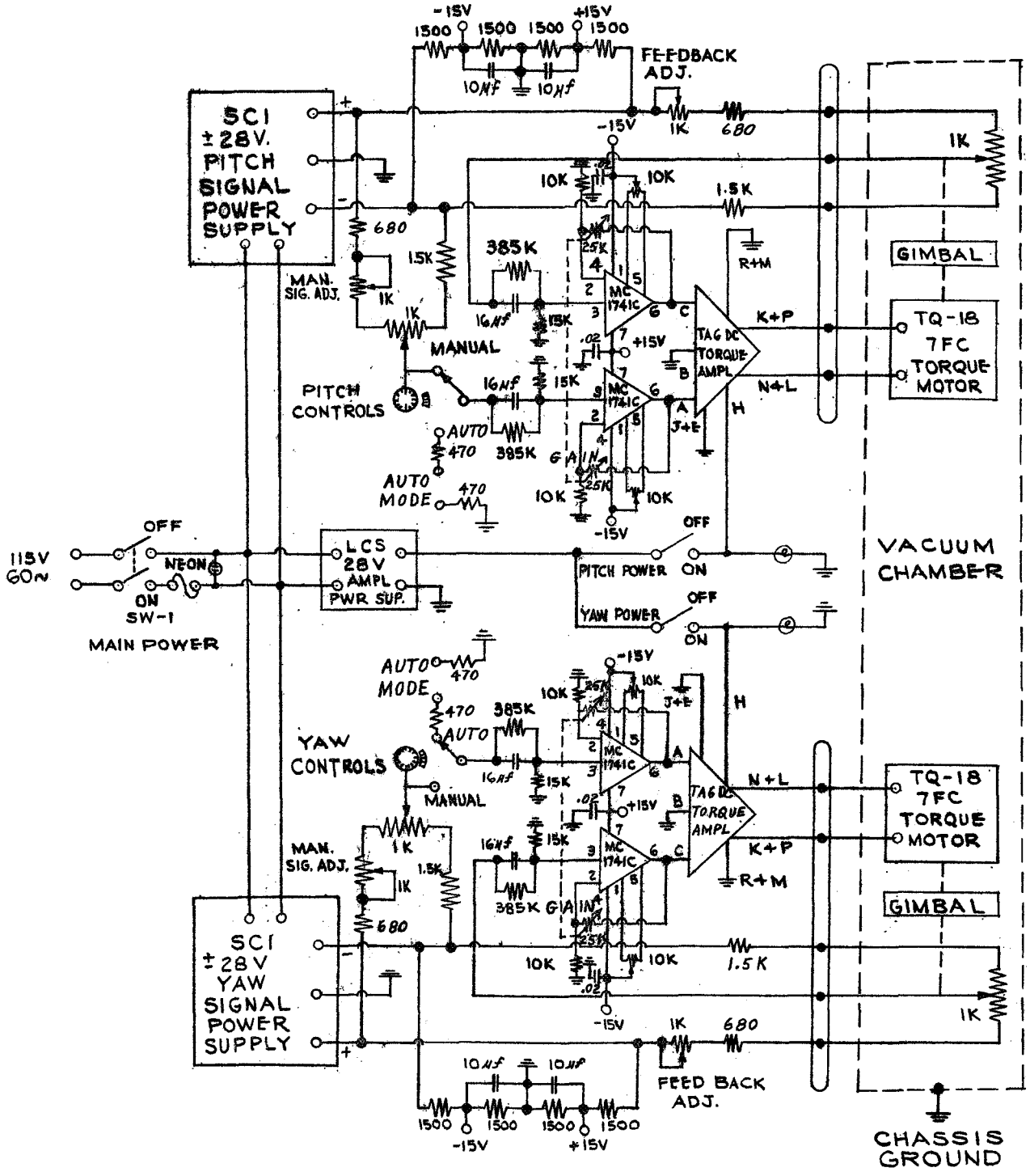

Figure 13. Gimballed detector control unit schematic.

85°C. The actual electrical travel is 352° ± 2°. The starting torque and running torque are listed as being 0.15 oz-in. max. The life expectancy is 2 x 10^6 shaft revolutions. The minimum resistance increment is 1.52 ohms (for the 1K potentiometers under discussion) and the wire temperature coefficient is +130 ppm/°C. The ambient temperature range goes from -65°C to +150°C.

The power supply used to furnish ±28 Volts to the torque amplifiers is a Lambda Model LCS-4-28 regulated supply.

The two power supplies used to furnish the dc feedback voltages, manual control signal voltages and operational amplifier power are Semiconductor Circuits, Inc., Model 2.28.100 dual output plug-in power supplies. Regulation is .01% for line and .05% for load. Ripple is 1 mV. max RMS, temperature coefficient is .02%/°C typical and operating temperature range is -25°C to +71°C. They are short circuit protected.

The operational amplifiers that were used to isolate the phase lead filters and the torque amplifiers, as well as to provide additional gain as required, were Motorola Model MC 1741CG amplifiers. These units can handle a differential input signal of ± 30 volts max. The gain can be varied by changing the feedback resistor, maintaining a low output impedance of the order of 300 ohms and a high input impedance of 300 K ohms or greater. These amplifiers have an operating temperature range of 0 to +75°C and they feature short circuit protection, no frequency compensation required, offset voltage null capability, wide common mode and differential voltage ranges and low power consumption.

Figure 14 is a photograph of the gimballed detector control unit. The sloping front panel with the manual positioning controls are visible together with the relatively large torque amplifier power supply and one of the small Aeroflex Laboratories torque amplifiers.

Signal Processing Electronics

The design of the signal processing electronics is based primarily on the use of available integrated circuits for minimum weight and power. The A/D converter is a single integrated circuit that includes all the necessary functions except the comparator and resistor ladder network, which are two separate packages. All of the other logic functions use the very low power complementary symmetry MOS integrated circuits.

A block diagram of the complete unit is shown in Fig. 3. The logarithmic electrometer is included to provide a signal to the A/D converter for demonstration purposes. It is not compensated and is not intended for operational use.

As in most digital systems, clock pulses are provided for timing the various logic functions and the clock operates at the bit rate frequency. The clock oscillator (IC 1, board 2) is an astable multivibrator operating at approximately 50 KHz.

The clock pulses are divided by ten in the A/D converter and then appear as an end of conversion pulse output. These ten bit word pulses are then divided by two (IC 2, board 2) for the multiplexer. The alternate pulses from the two outputs of this flip-flop are shaped to a shorter (approximately 20 μs) pulse length by two trigger circuits (IC 1 and IC 2, board 3) to trigger the "on" time of the two multiplexer MOS switches (IC 1, board 1). This completes the logic system.

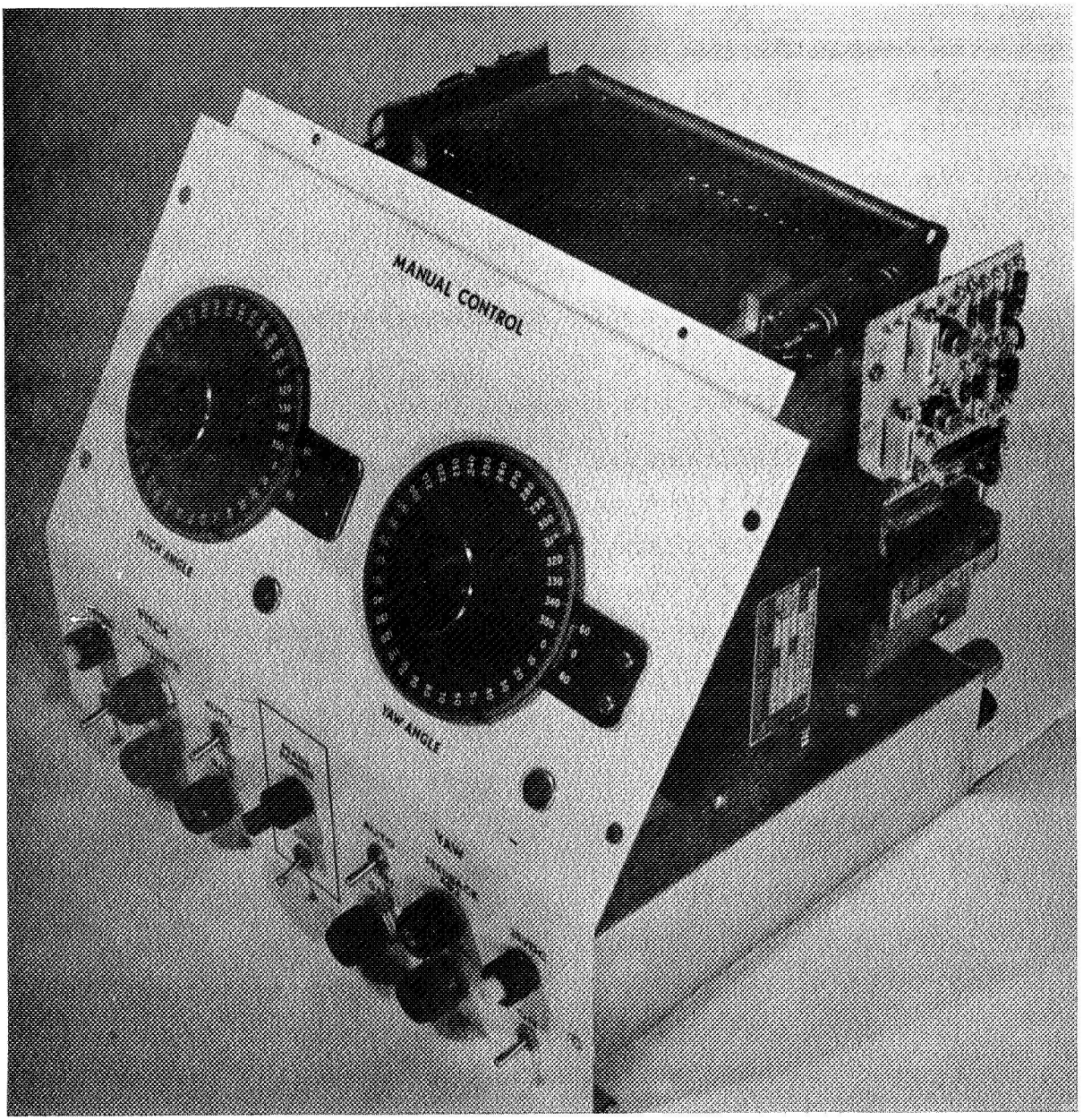

Figure 14. - Photograph of Gimballed Detector Control Unit.

The power supply is a standard dc to dc converter with a pre-regulator. Outputs include regulated ± 15 V, - 5 V for the reference voltage, and -27 V for the A/D converter.

All of the signal processing electronics are mounted on five printed circuit boards divided as shown in the schematic diagrams of Figures 15 and 16. The five boards are mounted in an aluminum box 1½ x 2½ x 4 inches. The electrometer board, which includes the multiplex switches, is at one end of the box with a shielding partition separating it from the rest of the circuitry. The dc to dc converter chopper is mounted at the opposite end to reduce any possible coupling with the electrometer at the chopper frequency.

The electrometer input is a Microdot coax connector. All of the other input and output leads are handled by a single 9 pin keystone connector. Available at the plug are the serial digital output, the clock frequency, frame and even frame pulses, and electrometer analog output. Power input is about 1.3 watts at 28 volts and the total weight is 12 ounces. Figure 17 is a photograph of the signal processing electronics package.

TESTS AND RESULTS

Consider first the response of a simple viscous damped servo control system to a sinusoidal input function. A schematic of such a simple servo system in which an output shaft is positioned to correspond with an input shaft position is shown in Figure 18. The equation of motion of this system is:

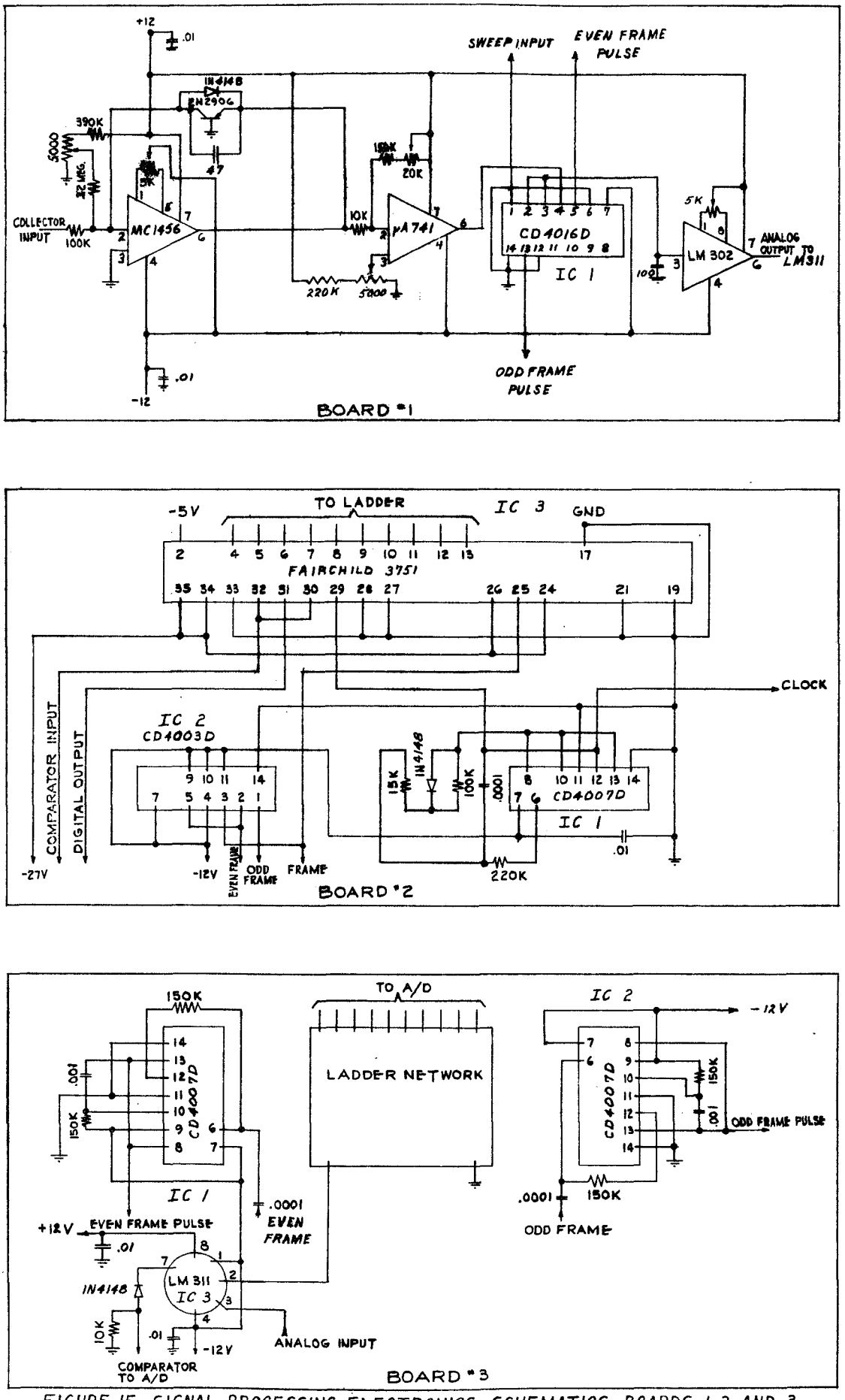

FIGURE 15. SIGNAL PROCESSING ELECTRONICS. SCHEMATICS, BOARDS 1, 2 AND 3

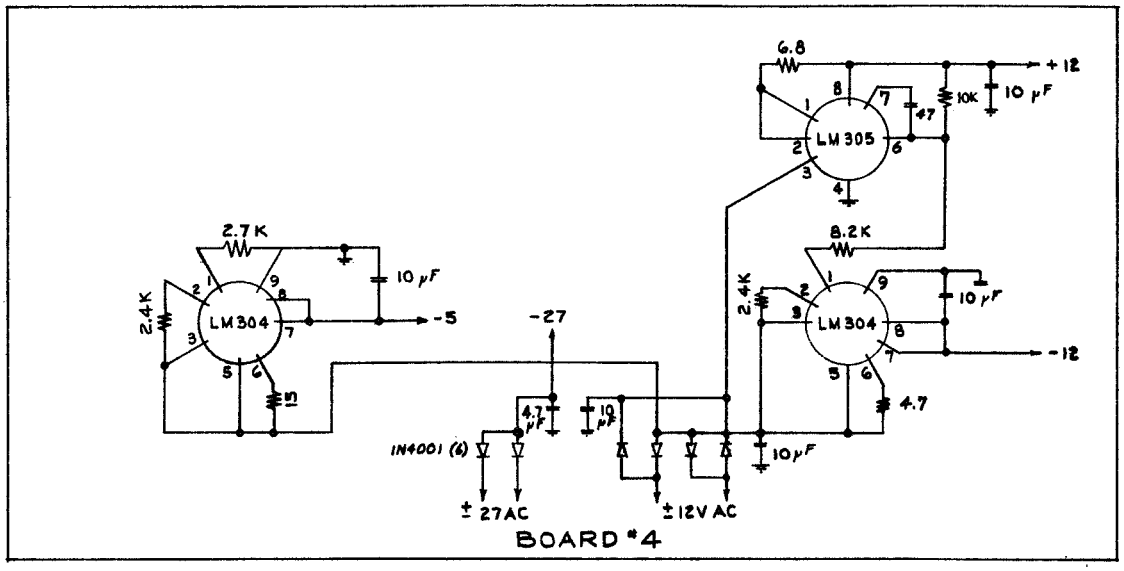

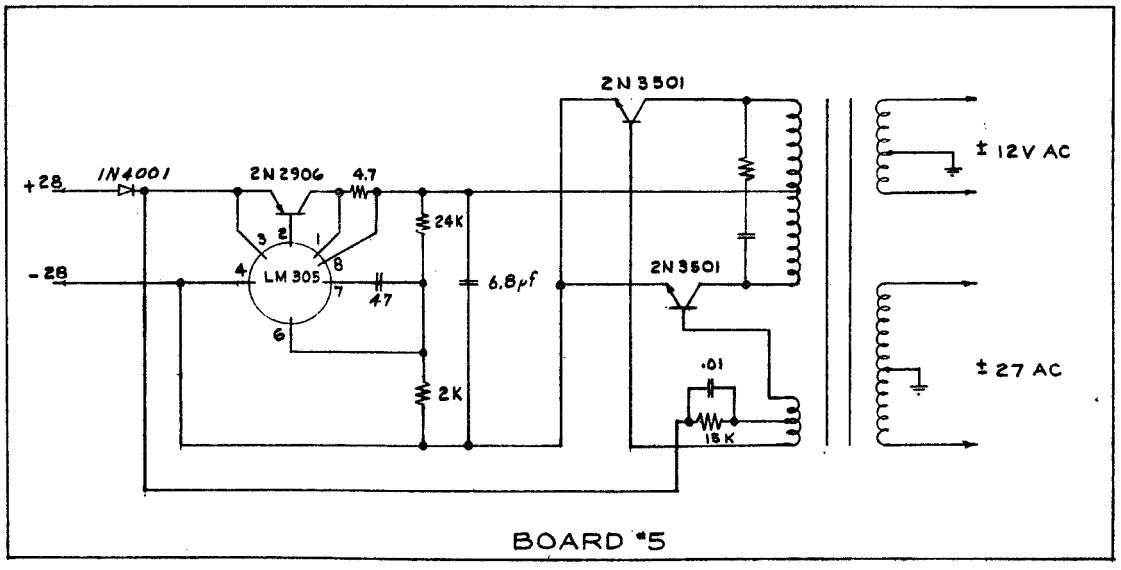

FIGURE 16. SIGNAL PROCESSING ELECTRONICS SCHEMATICS, BOARDS 4 AND 5

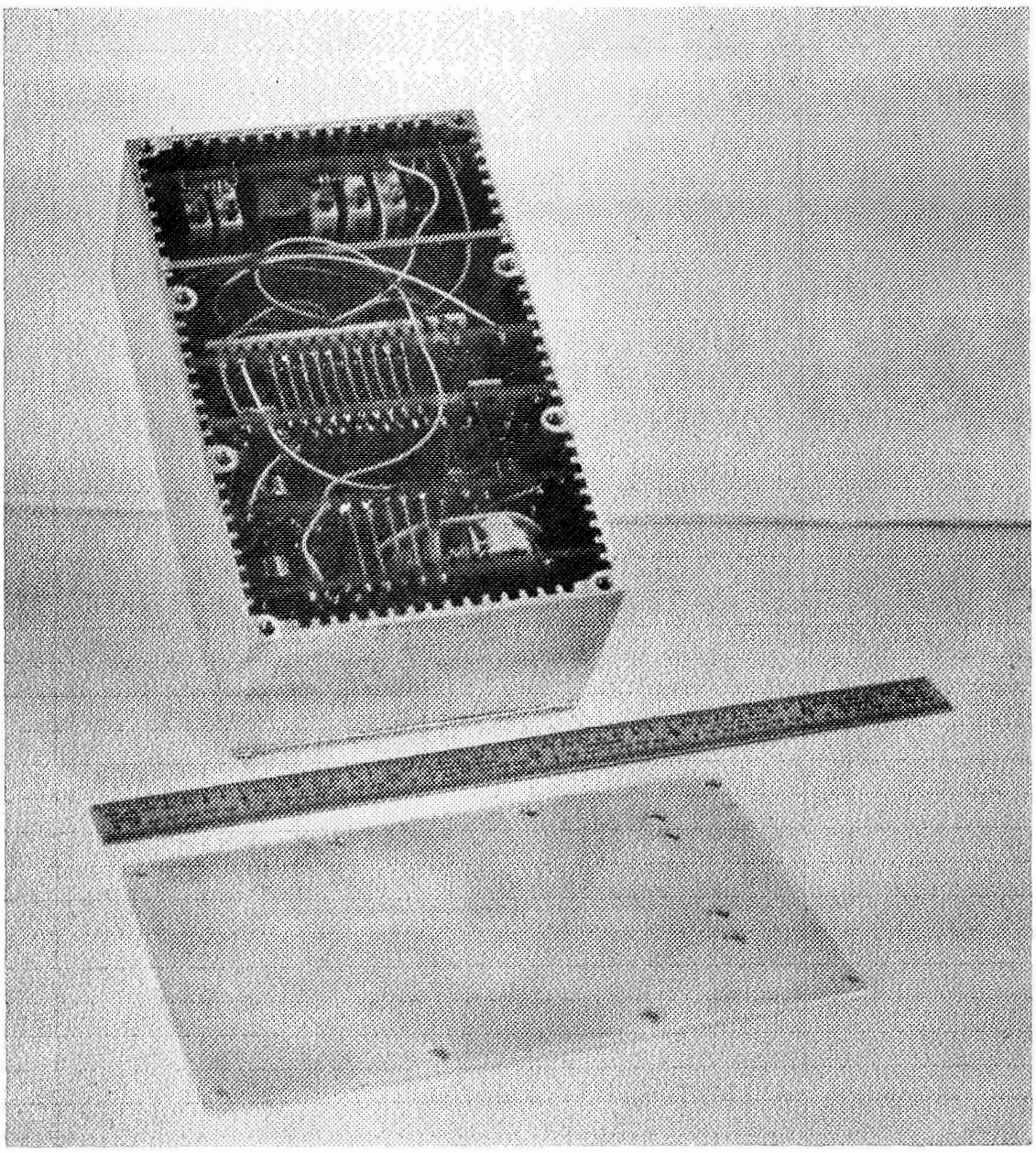

Figure 17. - Photograph of Signal Processing Electronics.

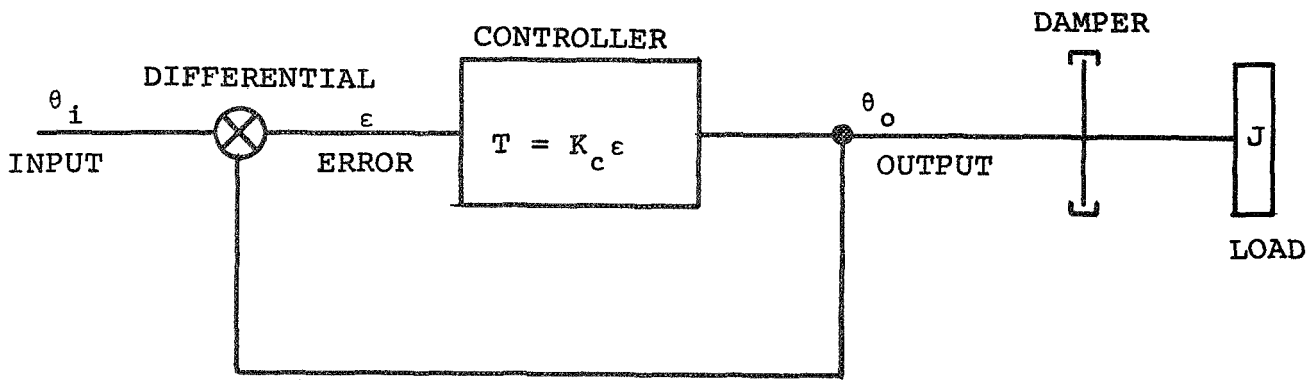

Figure 18. Simple Servomechanism with Viscous Output Damping

$$J \frac{d^2\theta}{dt^2} + F \frac{d\theta_o}{dt} = K_c \varepsilon = K_c(\theta_i - \theta_o)$$

or

$$J \frac{d^2\theta_o}{dt^2} + F \frac{d\theta_o}{dt} + K_c\theta_o = K_c\theta_i \qquad (1)$$

where ε is the error or difference between the output θ_o and the input θ_i angular positions. The input and output angles are usually expressed in radians, the controller torque constant K_c is given in dyne-cm/radian, the load moment of inertia J is given in $gm\text{-}cm^2$ and the friction torque per unit output speed F is given in dyne-cm per radian per second.

Let the input shaft position θ_i vary as a pure sinusoidal function of time with unit amplitude

$$\theta_i = \cos \omega t \qquad (2)$$

Then one expects that for a linear system the output shaft position will also vary sinusoidally with the same frequency but with a different amplitude A and phase λ as follows:

$$\theta_o = A \cos (wt + \lambda) \qquad (3)$$

Since $e^{jwt} = \cos \omega t + j \sin \omega t$, equations (2) and (3)

may be considered, respectively, as the real parts of the functions below:

$$\theta_i = e^{jwt} \tag{4}$$

$$\theta_o = A\, e^{j(wt+\lambda)} \tag{5}$$

Taking the first and second derivatives of equation (5) and substituting these expressions for θ_i, θ_o, $d\theta_o/dt$ and $d^2\theta_o/dt^2$ in equation (1) one obtains the expression:

$$A\, e^{j\lambda} = \frac{1}{1-\omega^2(J/K_c) + j\omega\,(F/K_c)} \tag{6}$$

Now, the moment of inertia J and the controller constant K_c are related to the resonant frequency ω_n of the servo according to the relationship:

$$\frac{J}{K_c} = \frac{1}{\omega_n^{\,2}} \tag{7}$$

Similarly, one can define a critical damping factor F_c which is related to J and K_c:

$$F_c = 2\sqrt{J\,K_c} \tag{8}$$

The damping factor F can be related to the critical damping F_c by means of the damping ratio c :

$$c = F/F_c \tag{9}$$

The ratio between F and K_c becomes:

$$\frac{F}{K_c} = \frac{2c}{\omega_n} \tag{10}$$

Equation (6) can then be written as

$$A\, e^{j\lambda} = \frac{1}{1 - (\omega^2/\omega_n{}^2) + 2\, jc\, (\omega/\omega_n)} \tag{11}$$

If we introduce the variable

$$d = \frac{\omega}{\omega_n} \tag{12}$$

we get the expression

$$A\, e^{j\lambda} = \frac{1}{1 - d^2 + j(2cd)} \tag{13}$$

which can be considered as representing a vector of magnitude A and phase angle λ (both relative to the input displacement taken as a unit reference vector) such that

$$A = \frac{1}{\sqrt{(1-d^2)^2 + 4c^2d^2}} \tag{14}$$

and

$$\lambda = - \tan^{-1} \frac{2cd}{1-d^2} \qquad (15)$$

Thus for an input function of the form

$$\theta_i = \cos \omega t , \qquad (2)$$

the output function θ_o can be written as:

$$\theta_o = \frac{1}{\sqrt{(1-d^2)^2 + 4\ c^2d^2}} \cos \left(\omega t - \tan^{-1} \frac{2cd}{1-d^2}\right) \qquad (16)$$

The value of the variable $d = \omega/\omega_n$ for which the output oscillation amplitude A is a maximum is found by differentiating equation (14) with respect to d and equating to zero. The result is:

$$d_{Amax} = \sqrt{1-2c^2} \qquad (17)$$

The resulting maximum amplitude is:

$$Amax = \frac{1}{2c\sqrt{1-c^2}} \qquad (18)$$

Expressions (17) and (18) have physical significance only for values of c that are smaller than $1/\sqrt{2}$ since for $c > 1/\sqrt{2}$ there is no maximum.

In order to experimentally measure the parameters of a viscous damped servo control system, the input member of the system is displaced back and forth with constant amplitude Ain and gradually increasing frequency. The maximum oscillation amplitude $A_{out\ max}$ of the output member is measured, as well as the input frequency ω_{Amax} at which this maximum occurs.

The value of the damping ratio c may then be calculated from euqation (18) written in the form:

$$c = \sqrt{\frac{1 - \sqrt{1 - (Ain/Aout\ max)^2}}{2}} \qquad (19)$$

The natural frequency ω_n of the system can be calculated from the value of c just found and the corresponding value of d as given by equation (17). It is equal to

$$\omega_n = \frac{\omega_{Amax}}{d_{Amax}} = \frac{\omega_{Amax}}{\sqrt{1-2c^2}} \qquad (20)$$

In place of the amplitudes of the input and output angles A_{in} and A_{out} one can measure the amplitudes of the equivalent input and output voltages and obtain the damping ratio c and the resonant frequency ω_n.

A second method of determining the resonant frequency ω_n is to compare the phases of the input and output displacements or voltages. The phase lag of the output with respect to the input becomes 90 degrees at the resonant frequency independent of the amount of damping and approaches 180 degrees for higher frequency values.

For a viscous damped servo system in which a phase lead or error-rate stabilization network has been included, the system will have combined viscous output damping and error-rate damping. The equation of motion for this case is more complex since it contains an additional term and the solutions contain two damping parameters instead of a single parameter. It is best to analyze the performance of such systems on the basis of a comparison between the theoretical and experimental closed loop frequency responses and the response to a step input function.

The theoretical closed loop frequency response of the redesigned servo system was presented in Figure 9. As a comparison, the experimental closed loop frequency response of the redesigned servo system is shown in Figure 19. Comparing the resonant frequencies and the bandwidths, we see that the actual servo system has a slightly larger resonant frequency and bandwidth than the ideal theoretical servo. The gain at the resonant frequency is slightly smaller for the actual servo than for the theoretical servo even though the actual servo amplifier gain of 1.37 is greater than the theoretical servo gain of 1.0..

The equipment that was used to test the gimballed detector servo system consisted of a Krohn-hite Instrument Corp. Ultra-Low Frequency Oscillator Model 400-A,which can furnish either a sine wave or square wave signal,and two Moseley Autograph Model 680 strip chart recorders to record the input signal and the output response of the servo system. These strip chart recorders have a full scale balance time of 1/2 second

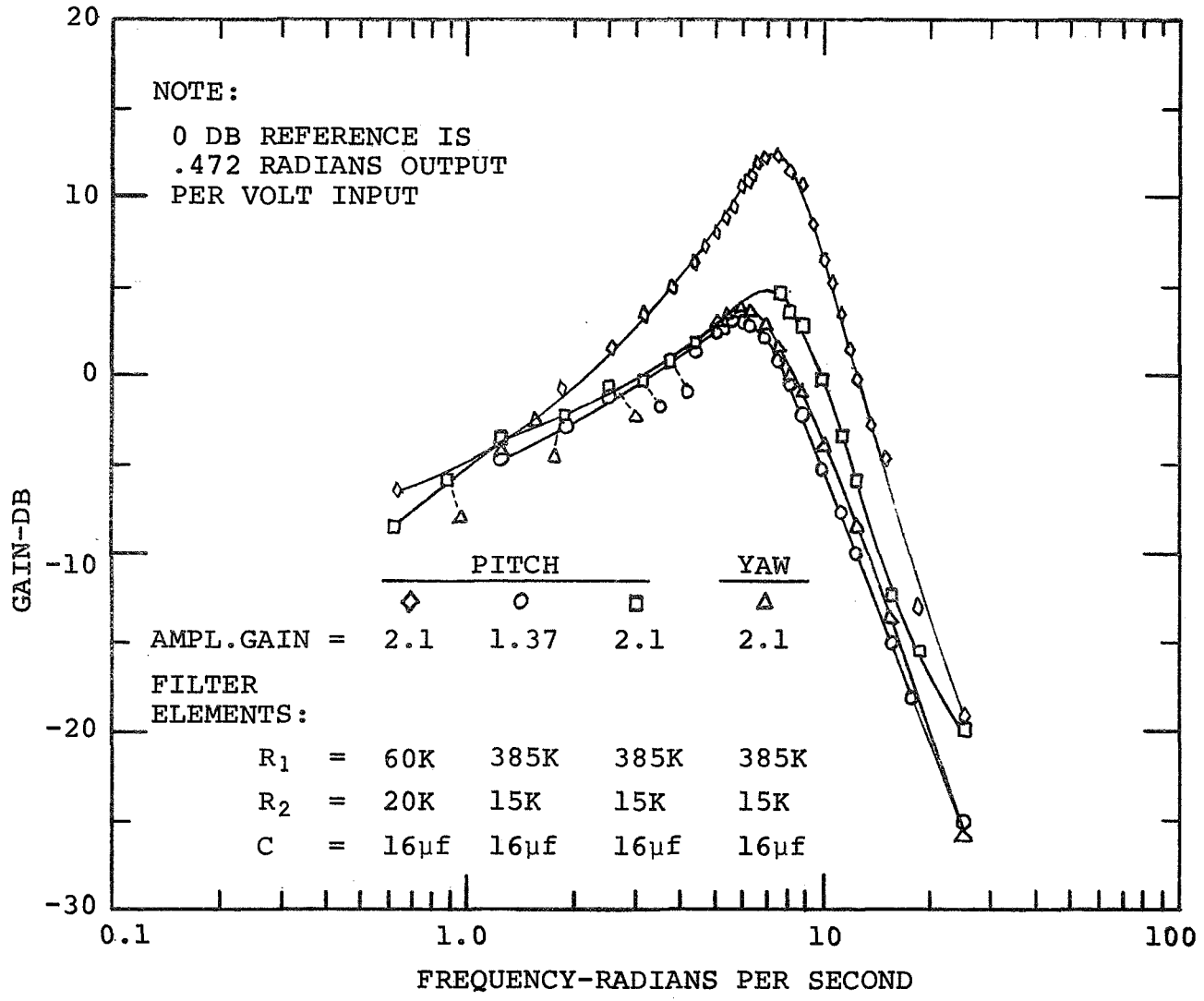

Figure 19. - Experimental Closed Loop Frequency Response of the System.

and could be used with frequencies up to 2.5 cps without appreciable attenuation. The accuracy and resolution of the recorders is said to be 0.2% of full scale with 0.1% of full scale resettability.

The input test signal to the servo system was monitored at the input of the signal channel filter. The sine wave test signal remained relatively constant in amplitude over the entire frequency range covered from 0.1 cps to 2.4 cps. The output response of the servo system was monitored at the feedback potentiometer which follows the motions of the simulated detector (and connects to the input of the feedback channel filter).

The servo system response to a step input function was measured by using two separate regulated power supplies to furnish two separate input voltages and switching the filter input from one voltage to the other. The output response of the system was measured at the feedback potentiometer as before.

The effect of changing the gain of the operational amplifiers from 1.37 to 2.1 and changing the two filter resistors can be seen in the frequency response curves of Figure 19. It is obvious that the gain of the servo at the resonant frequency increases with the operational amplifier gain and that both the resonant frequency and the bandwidth increase as the gain increases. The theoretically calculated filter of

$$R_1 = 385K \text{ and } R_2 = 15K$$

provides an improved frequency response without too much underdamping. The pitch response is somewhat better than the yaw response because of the added moment of inertia of the gimbal.

The pitch response of the redesigned servo system (with an operational amplifier gain of 1.37) to a step input function is shown in Figure 20. The transient overshoot was 25 percent. The transient rise time T_R was 0.35 seconds. The time to reach peak value T_p was 0.64 seconds. The actual damping of the system was such that there were no successive undershoots and overshoots.

In addition to the servo system dynamic response tests detailed above, other tests were made to determine other characteristics of the system. For example, the accuracy of machining of the various components was verified when the simulated detector and the attached spherical detector head were aligned so that a uniform .005" gap existed between the detector head and the housing head. The detector moved freely inside the housing cylinder within a total range of $\pm$ 25 degrees in pitch and yaw as designed.

The detector was tested for static balance and was found to be well balanced in both pitch and yaw so that it remained motionless in any position.

The vacuum tightness of the enclosed housing assembly was verified with both the top and bottom view caps cemented in position with Torr Seal epoxy.

The static friction torque of the pitch potentiometer, bearings and connecting wires was determined by placing increasing weight on the detector at a fixed distance from the central pivot point until the detector began to move. The pitch static friction torque was found to be .092 oz-in, considerably smaller than the maximum static torque listed for the potentiometer (.15 oz-in.).

The weight of the gimbal, gimbal mount, simulated detector with its spherical head and the housing head was 5 1/8 lbs. The cylindrical housing case weighed 3 1/8 lbs.

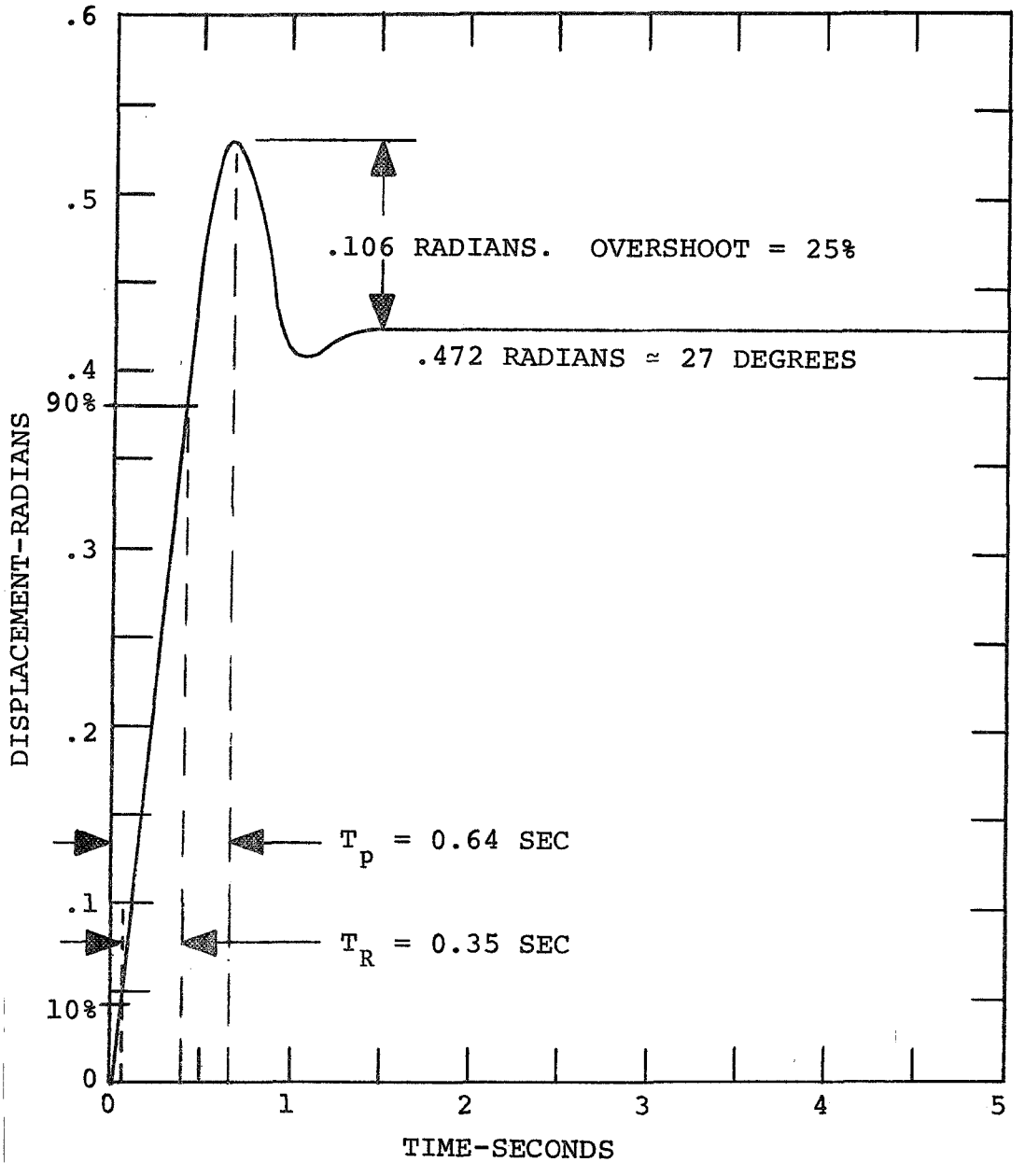

Figure 20. - Experimental System Response to a 0.9 Volt Step Input.

Finally, the average deviation between the manual control position and the detector position in the manual mode for a series of transient movements of the manual control was measured to be $\pm$ 1.1 degrees, with the operational amplifier gain set at 2.1 and the theoretically calculated filter in use.

In order to test the performance of the signal processing electronics, a D/A converter and demultiplexer were constructed on a single circuit board. These circuits provide two analog outputs corresponding to the multiplexed digital input. By comparing the analog input to the digitizer to the analog output of the test board, the overall system performance can be demonstrated. Figure 21 is an X-Y recording of the input and output signals of one channel and shows the excellent linearity of the system. Because the reference for the commercial D/A converter is 10 volts, the output (nominally equal to 5 volts) has been scaled to equal the input.

Cross talk between channels is less than 0.25% in the worst case - one channel 0, the other maximum. This is primarily due to the compromise in sampling time. A short sampling time is required to hold a fixed data point for the data conversion when the input is changing. Longer sampling times will improve the cross talk but will introduce error in the data conversion process.

Unfortunately, an operating quadrupole mass spectrometer was not available to test the unit under operating conditions. However,the tests that were made indicate that satisfactory operation should be obtained.

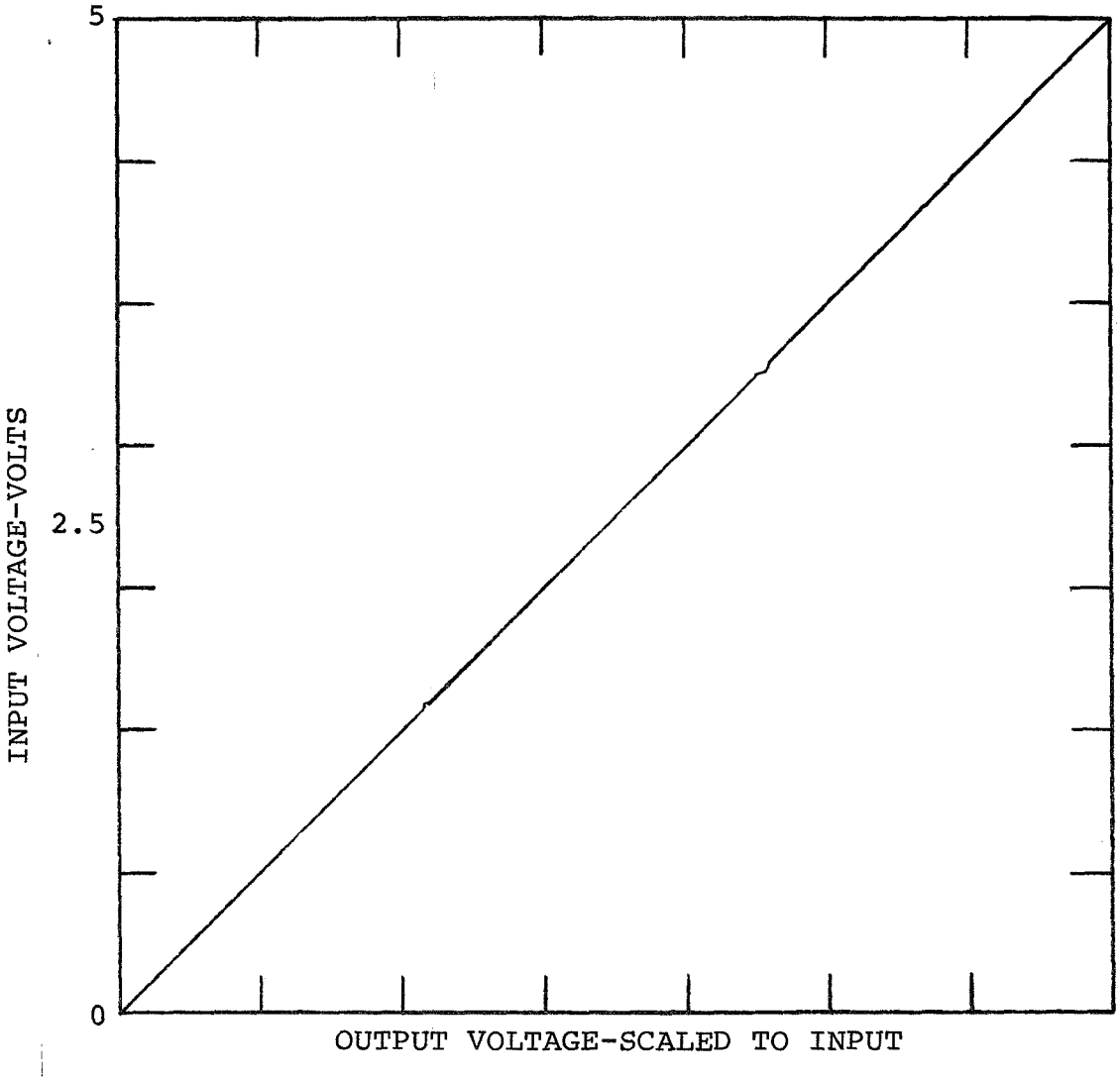

Figure 21. - Input Voltage Vs. Decoded Output Voltage.

CONCLUSIONS AND RECOMMENDATIONS

The many tests that were made to determine the performance of the gimballed detector servo system show that the system behaved approximately as designed. The experimental and theoretical performance do not agree exactly because the actual system departed somewhat from the idealized assumptions of the theory. For example, the theoretical model did not take into account the static and running friction of the wire-wound potentiometers and the ball bearings, nor did it consider the decreasing torque of the brushless dc motor for angular departures from the zero position. The friction affected the low frequency performance of the system, causing the attenuation shown in Figure 19 at frequencies well below resonance. Friction also helped reduce the gain at the resonant frequency (an operational amplifier gain of 1.37 instead of 1.02 as calculated theoretically was required to obtain a gain of about 3.0 db at resonance). The decreasing torque of the motor also helped reduce the gain at resonance.

Other departures from the theoretical assumptions involved the motor viscous damping, the settings of the feedback potentiometers and the moment of inertia of the simulated detector. The value chosen for the motor viscous damping corresponded to a zero source impedance. Since the output impedance of the torque amplifiers is some small, finite value, the actual viscous damping of the motor would be less than the assumed value. The total resistances of the feedback potentiometers were less than the nominal value of 1K and the feedback circuits were adjusted to yield about 2.12 radians/volt instead of 2.29 radians/volt as assumed. The moment of inertia of the simulated detector was not measured.

The theoretical frequency response curve of Figure 9 shows a resonant frequency at 5.5 rad/sec and a bandwidth of 8.4 rad/sec. The experimental response curve (with an operational amplifier gain of 1.37 instead of 1.02) shows a resonant frequency at 5.8 rad/sec and a bandwidth of 9.0 rad/sec.

In the step input function test, the experimental data yielded an overshoot of 25 percent compared with a theoretical value of about 40 percent. The measured time to reach the peak value was 0.64 seconds compared with the theoretical value of 0.40 seconds. Part of the difference between these values was undoubtedly due to the potentiometer and ball bearing friction. Part of the difference may also be due to the limited response speed of the strip chart recorders that were used. The lack of "ringing" in the measured step response clearly indicates the effect of the friction. The average deviation of 1.1 degrees between the manual position control and the actual position of the simulated detector also demonstrates the effect of the system frictional forces.

Summarizing the conclusions, one can make the following statements:

1. It is possible to build a gimballing system out of aluminum and stainless steel that is small in size, light in weight, low in power, has a low vacuum conductance spherical seal at the front so that it is essentially vacuum enclosed, has angular position accuracies of the order of 1 degree and a speed of response of the order of 1 second.

2. Brushless, limited angle dc torque motors are quite suitable for this application.

3. Precision, wire-wound feedback potentiometers function properly in this application. However, they do limit the resolution to about 0.5 degrees because of the discrete resistance steps. In addition, their starting and running friction torques of the order of 0.1 oz-in. limits the system accuracy to about 1 degree and degrades the system performance somewhat.

4. A phase lead filter can be designed to improve the system performance.

5. Coiled magnet wire can be used to make connections to the moving detector without introducing significant damping or torque.

Although the wire-wound potentiometers used in this project were standard components, it is possible to obtain these same potentiometers with a proprietary dry film lubricant for vacuum service. The effect of such a dry film lubricant on the system performance is expected to be small. However, such a lubricant is recommended for extended vacuum operation of the system.

It is recommended that further work be performed in the following areas:

1. Redesign some of the gimbal system components to make them lighter.

2. Develop a pyrotechnic operated break-off seal to cover the front end of the gimballed detector.

3. Investigate the possibility of replacing the wire-wound feedback potentiometers with either synchro repeater type feedback elements or lower torque continuous-strip resistance type potentiometers.

4. Test the response of the system over a wide range of temperatures in a vacuum environment.

REFERENCES

1. Hueser, J. E., and Brock, F. J., Final Report, NASA Contract No. NAS1-5347-15.

2. Sagalyn, R. C. and Smiddy, M., "Positive Ion Sensing System for the Measurement of Spacecraft Pitch and Yaw, Air Force D-10 Experiment Flown on Gemini X and XII", AFCRL-67-0158, Dec. 1967, Air Force Surveys in Geophysics, No. 201.